

**DECELLULARIZED EXTRACELLULAR MATRIX- AGAROSE HYBRID BIOINK
DEVELOPMENT FOR 3D BIOPRINTING APPLICATIONS**

by

İPEKNAZ ÖZDEN

Submitted to the Graduate School of Engineering and Natural Sciences in partial fulfillment
of the requirements for the degree of Master of Science

Sabanci University

2018

DECELLULARIZED EXTRACELLULAR MATRIX- AGAROSE HYBRID
BIOINK DEVELOPMENT FOR 3D BIOPRINTING APPLICATIONS

APPROVED BY:

Prof. Dr. Bahattin Koç
(Thesis Supervisor)



Prof. Dr. Batu Erman



Prof. Dr. Gamze Torun Köse



DATE OF APPROVAL: 31/07/2018

© İpeknaç Özden, 2018

All Rights Reserved

İPEKNAZ ÖZDEN

MAT, M.Sc. Thesis, 2018

Thesis Supervisor: Prof. Bahattin Koç

ACKNOWLEDGEMENTS

Firstly, I would like to thank my supervisor, Prof. Dr. Bahattin Koç, for giving me the opportunity to improve myself as a scientist. I was privileged enough to have his guidance during these past 2 years. He has not only supported me academically but also he encouraged me to improve myself on other means. I also would like to thank Prof. Dr. Batu Erman and Prof. Dr. Gamze Köse for accepting to be my thesis committee members.

I would like to thank Sabanci University for supporting me financially and providing a homelike, warm environment during my studies.

I thank Koç group members; Mine Altunbek, Ali Nadernezhad, Özüm Çalışkan and Ferdows Afghah for always being open to my questions. I also thank the NS 101 team for helping me grow mature and confident.

I thank Kerem Yıldırım for his great moral support, my roommate Adea Gafuri for always inspiring me to work harder, Zain Fuad for widening my perspective, Ayk Telciyan for his friendship. I also would like to express my gratitude to Matjaž Moser for always motivating me to do better.

Last but not least, I would like to express my love and appreciation to my parents for being as supportive and patient as always.

ABSTRACT

Natural and synthetic biomaterials have been widely used in tissue engineering applications, but these materials lack the functional, mechanical, biological and structural complexity of natural extracellular matrix (ECM). Because reaching such complexity with ECM substitutes is very challenging, using the natural ECM itself as biomaterial in tissue engineering applications has gained much interest. As remnant cellular content from allogenic or xenogenic sources could cause unwanted host response, ECM needs to be decellularized before being used as biomaterial.

Conventional tissue engineering approaches do not exhibit the necessary complexity and precision, and hence 3D bioprinting is used to create 3-dimensional structures with desired complexity and precision. Up to now, many biomaterials have been used as bio-inks for 3D bioprinting, but as they lack the necessary complexity, there is a need for novel bioinks. Decellularized extracellular matrix (dECM) is a great candidate to be used as bioink in 3D bioprinting as it provides the necessary microenvironments during and after bioprinting if it can be processed into a printable form.

This thesis work aims to create a novel bioink by combining cell sheet derived decellularized extracellular matrix (dECM) with a natural hydrogel, agarose. The cell sheets were decellularized and characterized before used as a bioink. The decellularization protocol and its effects on the structure of the extracellular matrix were evaluated. The dECM was solubilized, neutralized, mixed with 3T3 fibroblast cells and agarose before bioprinting. The blend bioink was bioprinted and cultured for a week. The results showed that the developed decellularization protocols were successful in terms of cellular removal and structural preservation. Also, the hybrid bioink provided an appropriate environment for cellular viability and microenvironment.

ÖZET

Doğal ve sentetik biyomalzemeler doku mühendisliği uygulamalarında günümüze kadar sıklıkla kullanılmış olsa da, bu malzemeler doğal ekstrasellüler matriksin sahip olduğu fonksiyonel, mekanik, biyolojik ve yapısal özellikleri taşımamaktadır. Alternatif malzemelerle bu özelliklere ulaşmak zor olduğundan, ekstrasellüler matriksin kendisi, doku mühendisliği uygulamalarında kullanmaya başlamıştır. Ekstrasellüler matriks, biyomalzeme olarak kullanılmadan önce hücresel içeriğinden arındırılmalıdır. Böylelikle, allojenik veya zenojenik kaynaklardan gelebilecek, istenmeyen reaksiyonlar önlenmiş olur.

Geleneksel doku mühendisliği yöntemleri, ihtiyaç duyulan hassasiyeti ve özellikleri taşımadığından, 3-boyutlu biyobasım yöntemi bu sorunları aşmak amacıyla sıklıkla kullanılmaktadır. Günümüze kadar pek çok malzeme, biyomürekkep olarak kullanılmış olsa da, arzu edilen özelliklere ulaşmadıklarından yeni biyomürekkeplere ihtiyaç duyulmaktadır. Hücresizleştirilmiş ekstrasellüler matriks, sahip olduğu özellikler nedeniyle biyomürekkep olarak kullanılmak için uygun bir adaydır.

Bu tez çalışmasında, hücre tabakası yöntemi ile üretildikten sonra hücresizleştirilmiş ekstrasellüler matriks yapılarını agaroz ile karıştırarak yeni biyomürekkep üretimi amaçlanmıştır. Hücresizleştirme yöntemlerinin üretilen yapılar üzerindeki etkileri ve yöntemin hücre uzaklaştırmadaki başarısı değerlendirilmiştir. Elde edilen yapılar, jelleştirilmiş, nötralize edilmiş, agaroz ve 3T3 fibroblast hücreleri ile karıştırılarak biyobasımları gerçekleştirilmiştir. Biyobasım sonrasında 1 haftalık inkübasyon gerçekleştirilmiştir. Alınan sonuçlar, geliştirilen hücresizleştirme yöntemlerinin hücre uzaklaştırmada başarılı olduğunu ve malzemenin yapısına zarar vermediğini göstermiştir. Ayrıca, üretilen biyomürekkebin hücre canlılığı için uygun ortam sağladığı olduğu görülmüştür.

To my lovely family

TABLE OF CONTENTS

ACKNOWLEDGEMENTS	iv
ABSTRACT	v
ÖZET.....	vi
LIST OF FIGURES	x
1. INTRODUCTION.....	1
1.1. Biomaterials Used In Tissue Engineering	1
1.1.1. Synthetic biomaterials used in tissue engineering.....	1
1.1.2. Natural biomaterials used in tissue engineering.....	2
1.2. Extracellular Matrix (ECM).....	4
1.2.1. Sources of ECM	4
1.2.2. Structure, functions, and applications of ECM as a biomaterial.....	7
1.2.3. Production steps of ECM biomaterials	10
1.3. Decellularization Process.....	10
1.3.1. Purpose of decellularization and success criteria in decellularization.....	10
1.3.2. Decellularization techniques	12
1.3.3. Decellularization methods.....	12
1.4. 3D Bioprinting.....	14
1.4.1. Bioprinting methods	15
1.5. Bioinks used for 3D Bioprinting Applications.....	20
1.5.1. dECM as bioink for 3D bioprinting applications	21
2. EXPERIMENTAL	23
2.1. Fibroblast Cell Culture	23
2.2. Fibroblast Cell Sheet Culture.....	24
2.3. Preparation of Decellularization Agents.....	25

2.4.	Decellularization of Fibroblast Cell Sheets	25
2.5.	Evaluation of Decellularization Protocol.....	26
2.5.1.	Genomic DNA assay	26
2.5.2.	DAPI staining.....	27
2.5.3.	F-actin immunostaining	27
2.6.	Characterization of dECM	28
2.6.1.	Collagen I immunostaining.....	28
2.6.2.	Fourier-Transform Infrared (FT-IR) spectroscopy analysis	28
2.7.	Preparation of dECM Hydrogel	29
2.7.1.	Solubilization of dECM powder.....	29
2.7.2.	Neutralization and sterilization of dECM solution.....	30
2.8.	Preparation of Cell Laden dECM- Agarose Hybrid Bioink.....	31
2.9.	Bioprinting of Cell Laden dECM- Agarose Hybrid Bioink	32
2.10.	Live/Dead Assay	34
3.	RESULTS & DISCUSSIONS	36
3.1.	Fibroblast Cell Sheet Culture and Decellularization of Fibroblast Cell Sheets.....	36
3.2.	Evaluation of Decellularization Protocol.....	37
3.2.1.	Genomic DNA assay	37
3.2.2.	DAPI staining and F-actin immunostaining.....	38
3.3.	Characterization of dECM	39
3.3.1.	Collagen I immunostaining.....	39
3.3.2.	Fourier-Transform Infrared (FT-IR) spectroscopy analysis	41
3.4.	Live/Dead Assay	45
4.	CONCLUSION AND FUTURE WORK.....	48
	REFERENCES	50

LIST OF FIGURES

Figure 1: Processing of ECM derived from tissues (A) ECM-based hydrogel scaffolding, (B) ECM-based electrospinning, (C) Tissue 3D bioprinting [24]	5
Figure 2: Processing of ECM derived from cell culture (A) ECM surface modification, (B) ECM scaffold from resolvable polymer master, (C) Cell sheet assembly [24].....	7
Figure 3: ECM structure, summarized [33]	8
Figure 4: 3 main bioprinting methods summarized, (a) Micro-extrusion printer, (b) Inkjet printer, (c) Laser direct writing [53]	16
Figure 5: Widely used commercial bioprinters. (a) NovoGen 3D Bioprinting Platform of Organovo, (b) Bioplotter of EnvisionTec, (c) 3D Discovery by RegenHU [47]	17
Figure 6: Fibroblast cell sheet culture (a) 3T3 fibroblast cells were seeded with 8000 cells/cm ² density in 6 well plates, (b) Cells were cultured for 5 weeks, (c) After 5 weeks cell sheets were detach from the surface	24
Figure 7: Steps of production of dECM gel (a) The dECM powder was obtained after freeze drying, (b) The dECM powder was digested with pepsin solution for 26 hours, (c) The digested dECM after 26 hours.....	30
Figure 8: Organovo bioprinter parts shown	32
Figure 9: Bioprinting steps explained (a) System elements shown, (b) Capillary and plunger enters the bioink reservoir, (c) Aspiration of the bioink, (d) Bioprinting on the printing stage	33

Figure 10: Bioprinted structures (a) Single stripe, (b) Three stripes printed next to each other	34
Figure 11: The DNA content comparison between non-decellularized samples (control) and decellularized samples (dECM).	37
Figure 12: Cell sheet structure observed after DAPI and F-actin staining.	38
Figure 13: DAPI and F-actin staining of both decellularized and non-decellularized samples (a) DAPI staining for control sample, (b) F-actin staining for control sample, (c) Merged image for control sample, (d) DAPI staining for dECM sample, (e) F-actin staining for dECM sample, (f) Merged image for dECM sample.	39
Figure 14: Collagen and DAPI staining of control and dECM samples (a) DAPI staining for control sample, (b) Collagen staining for control sample, (c) Merged image for control sample, (d) DAPI staining for dECM sample, (e) Collagen staining for dECM sample, (f) Merged image for dECM sample.	40
Figure 15: Cross-sectional images of DAPI and collagen staining (a) For control sample (b) for dECM sample.	41
Figure 16: FTIR spectrum for SDS.	42
Figure 17: FTIR spectrum for decellularized ECM (dECM).	42
Figure 18: FTIR spectra of SDS and dECM, merged (blue line represents dECM sample, green line represents SDS sample).	43
Figure 19: FTIR spectra of dECM and ECM control merged (blue line represents dECM sample, red line represents control sample)	44

Figure 20: Live/Dead Assay Day 0, (a) control (b) dECM.....	46
Figure 21: Live/Dead Assay Day 1, (a) control (b) dECM.....	46
Figure 22: Live/Dead Assay Day 7, (a) control (b) dECM.....	47
Figure 23: Quantification of Live/Dead Assay Results	47

1. INTRODUCTION

1.1. Biomaterials Used In Tissue Engineering

As the life quality and lifespan of humankind increases, there is a growing need for organ and tissue transplantation. Even though there are major improvements on transplantation technologies and the success of the procedure is higher than ever, there are not enough donors to fulfill this growing need. Only one-third of the patients are lucky enough to receive matching organs or tissues from donors [1]. Therefore, there is an urgent need to create new tissues and organs which are not sourced from a donor. This can be achieved by using tissue engineering which is a multidisciplinary field combining medicine, engineering, material science and biology, focusing on the regeneration, repair, and replacement of tissues and organs which are damaged, diseased or malfunctioning [2], [3]. In order to create tissue-engineered organs and tissues, the appropriate biomaterials need to be used. To date, there has been a various number of materials, synthetic or naturally derived, used for this purpose. In the following sections, examples of such materials are explained in details.

1.1.1. Synthetic biomaterials used in tissue engineering

Synthetic biomaterials such as polycaprolactone, polyethylene glycol, polylactic acid and polyglycolic acid have been used for tissue engineering applications. Synthetic materials have the advantage of being reproducible [4]. They have good mechanical properties, and their properties can be well controlled during their production but, they usually lack the requisite biological cues and signaling molecules [4].

Poly(ethylene glycol) (PEG) is a biocompatible material which is created by the polymerization of ethylene oxide [5], [6]. It has strong mechanical properties, is not toxic or immunogenic but

is bioinert therefore is widely used as blends with bioactive materials [6]. This biomaterial was approved by Food and Drug Administration for biomedical use [7].

Polycaprolactone (PCL) is a synthetic biomaterial used widely for a variety of tissue engineering applications such as mechanical support for bioprinting applications. PCL has biocompatible and non-toxic properties, therefore, is widely preferred [7].

Poly(lactic co-glycolic acid) (PLGA), which is copolymer of poly glycolic acid and poly lactic acid, is a biocompatible synthetic biomaterial used for tissue engineering applications. During bioprinting applications, PLGA is used as a paper for stacking the cells [7], [8].

1.1.2. Natural biomaterials used in tissue engineering

Unlike synthetic biomaterials, natural biomaterials, also called hydrogels, have weak mechanical properties. The properties of natural materials vary based on their batch [9]. They contain biological cues which are crucial for the biocompatibility and bioactivity of the biomaterial. Examples of naturally derived biomaterials, used in tissue engineering applications are alginate, collagen, gelatin, and chitosan.

Agarose is a natural biomaterial which is classified based on its melting temperature. Depending on the hydroxyethylation of the material, its melting temperature changes [10]. Low melting temperature agarose is widely used in extrusion-based bioprinting applications as it gels at temperatures around 26- 30 °C [11]. Agarose is not a bioactive material and does not support cell adhesion, but it has the potential to be used as a blend with other materials. Agarose has been used blended with collagen for extrusion-based bioprinting applications [12]. However, agarose cannot be used with inkjet bioprinting as its low viscosity may lead to the clogging of the nozzle [13].

Alginate, or alginic acid, is a natural biomaterial derived from brown seaweed and is used for 3D bioprinting, especially for extrusion-based bioprinting applications due to its printability, biocompatibility, low cost, tunable viscosity, low toxicity and rapid gelation [5], [14], [15]. Due to its rapid gelation feature, alginate has good printability [6]. Unfortunately, alginate is a bioinert material, that is, due to its hydrophilic nature cells cannot interact with the material and cell proliferation, as well as migration, is limited [5].

Chitosan is a non-toxic, antibacterial and antifungal natural biomaterial widely used for wound healing purposes [6]. Chitosan has biodegradable properties, but it lacks mechanical strength, and hence, it is widely used as blends with other biomaterials [5].

Collagen is the most abundantly found protein in the animals [6]. Due to its arginine-glycine-aspartic acid (RGD) amino acid sequence, it helps cell attachment and proliferation, therefore, can be used as tissue scaffolds [16], [17], [4], [15]. When collagen is degraded hydrolytically, the resulting product is gelatin [18]. Gelatin is a biocompatible and non-immunogenic biomaterial which can be degraded completely *in vivo* [19]. It has low antigenicity, low cost and also contains RGD amino acid sequence which makes it a successful material for tissue engineering and cell attachment [20]. It is widely used for bioprinting applications in the form of Gelatin methacrylate (GelMA) which is a modified version of gelatin that can crosslink with UV light and has mechanical strength [21].

1.2. Extracellular Matrix (ECM)

Those synthetic and natural materials mentioned before lack the functional, mechanical, biological and structural complexity of natural extracellular matrix (ECM) therefore they cannot provide necessary cues to perfectly recapitulate the functions and structure of native tissues and organs [22]. As reaching such complexity with ECM constituents is very demanding, the solution is to use the natural ECM itself as a biomaterial for the tissue engineering applications.

1.2.1. Sources of ECM

1.2.1.1. Tissue-derived ECM

ECM derived from tissues have different properties based on the tissue of origin. As every tissue has their unique properties, the strengths and weaknesses of ECM obtained from different tissues are different. Therefore, the ECM should be obtained from a certain tissue depending on the requirement of use. ECM obtained from tissues are abundant in amount, but there are some drawbacks that lead scientists to prefer cell-derived ECM. Such drawbacks are the dependence of composition and structure of the material to the condition of the tissue source, the risk of pathogen transfer and unwanted host responses [23].

As can be seen in Figure 1, ECM derived from tissues can be further processed into different structures such as hydrogel, foam, fiber or they can be 3D printed. In order to produce hydrogels, ECM is first processed into particles. Then, with the help of digestive enzymes such as pepsin, it is digested and solubilized into hydrogel form. Same steps can be applied for foam formation. ECM fibers, on the other hand, are produced by electrospinning [24].

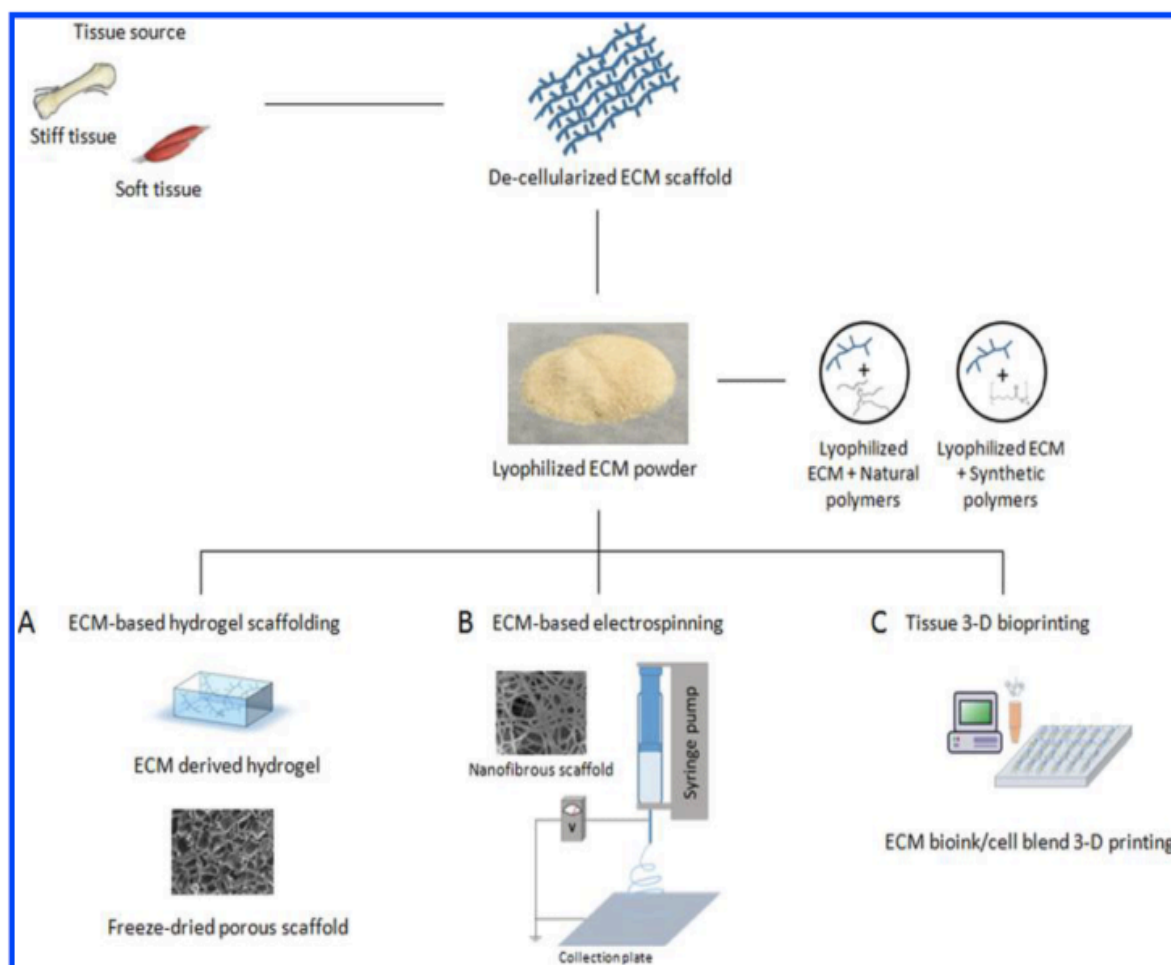


Figure 1: Processing of ECM derived from tissues (A) ECM-based hydrogel scaffolding, (B) ECM-based electrospinning, (C) Tissue 3D bioprinting [24]

1.2.1.2. Cell culture and cell sheet derived ECM

Although tissue-derived ECM has its advantages, the risk of pathogen transfer and host responses are great drawbacks. The ECM obtained from allogenic tissue sources might induce pathogen transfer while xenogenic ECM might cause unwanted host response [25]. In order to overcome these drawbacks and have a safer approach, ECM could be obtained from cell culture.

Cell-derived ECM reduce the risks of tissue derived ECM to a minimum and also has the advantage of great control over the product as cell-derived ECM properties can be altered by using different cell types, culture media, and culture systems as well as adding different

substrates. Moreover, the cell culture can be screened against pathogens. Autologous cells can be utilized as a cell source, which means overcoming the donor shortage problem [26], [27]. Another advantage of cell-derived ECM is ease of decellularization. The shortcomings of the cell-derived ECM are the long culture periods, increased cost due to the long culture period and weak mechanical properties [24]. Cell culture derived ECM can be used in many different forms for many different applications as can be seen in Figure 2.

Cell sheets can also be used as extracellular matrix sources and are created by culturing the cell types of interest for a long time, frequently on a thermo-responsive surface such as polydimethylsiloxane (PDMS) in order to easily remove the sheet from the surface with temperature variations. Cell sheets are dense stacks of cells created by long culture periods, and they possess an intact cell to cell attachment surrounded by the secreted extracellular matrix [28]. Cell sheets are removed from the surface without the use of proteolytic enzymes, therefore, their structure and integrity are preserved. Cell sheets possess many advantages such as controllable production period, ease of manufacturing and processing. Cell sheets can be created without the help of scaffolds and be transplanted without destructive applications such as suturing [29]. Cell sheet technology has been used for myocardial tissue engineering, corneal surface reconstruction, and periodontal applications [30]. The main drawback of cell sheet creation is the long culture period which leads to increased cost and contamination risk [24].

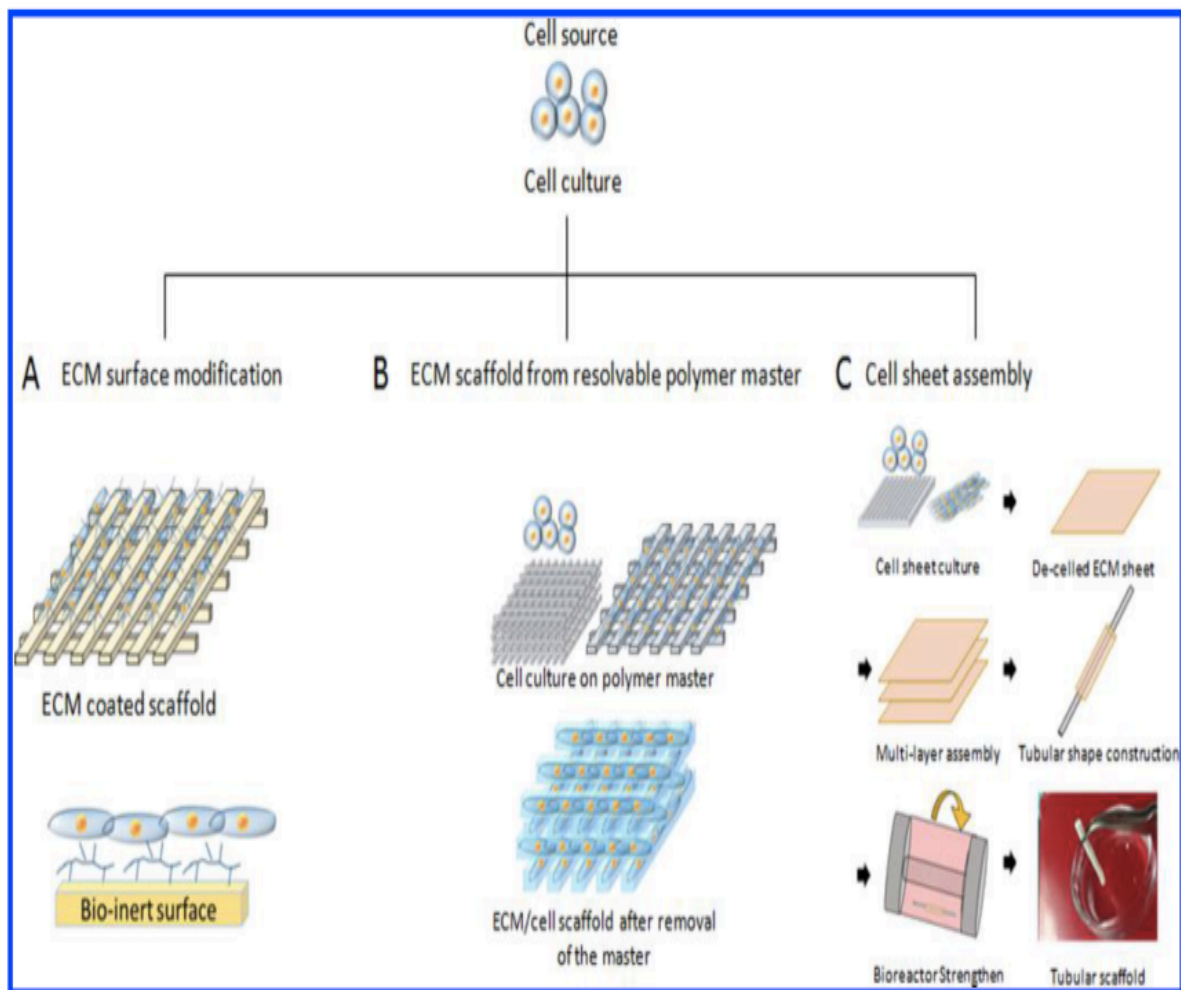


Figure 2: Processing of ECM derived from cell culture (A) ECM surface modification, (B) ECM scaffold from resolvable polymer master, (C) Cell sheet assembly [24]

1.2.2. Structure, functions, and applications of ECM as a biomaterial

The structure of ECM varies among tissues in a way that every tissue has different ECM structure providing the necessary microenvironment for the maintenance of the cells, a concept called organ specificity [31, 32]. Regardless of the tissue type, ECM structure is always composed of polysaccharides, proteins, growth factors and cytokines as shown in Figure 3.

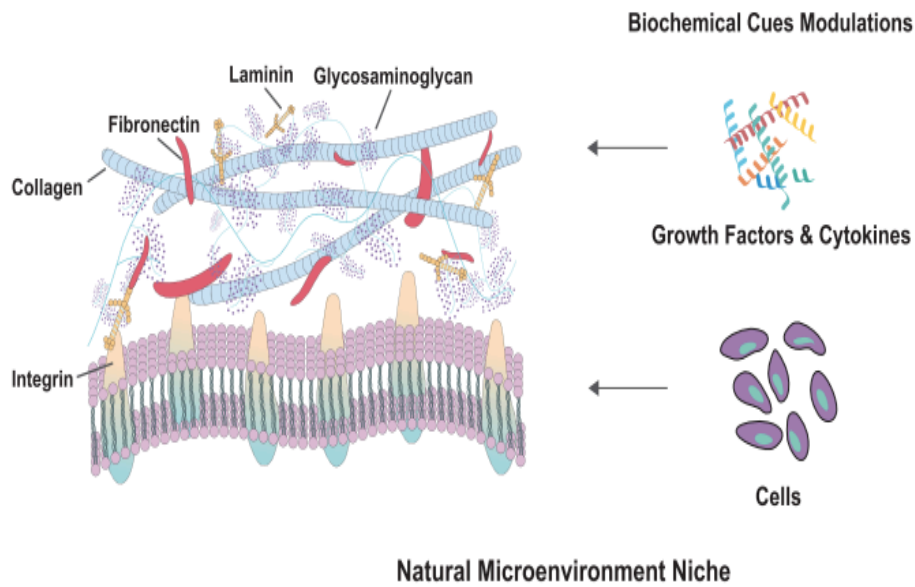


Figure 3: ECM structure, summarized [33]

Proteins found in ECM can have fibrous properties or adhesive properties. Fibrous proteins such as collagen and elastin provide structural support, elasticity and mechanical integrity to ECM while adhesion proteins such as fibronectin, laminin, and integrin keep other components of ECM intact and avail in cell proliferation, adhesion, and migration [24], [33].

Glycosaminoglycans are linear polysaccharides which carry a negative charge on their sulfate or carboxyl group, and hence, they can hold water molecules. This property provides mechanical stability to ECM and also engineered tissues as well [34].

ECM has a dynamic nature and responds to changes happening in the surrounding microenvironment. Its composition and activity change according to the environmental conditions and this concept is called dynamic reciprocity [35]. ECM influences cell differentiation, migration, proliferation [36].

ECM can be used in a reconstructive manner for tissue and organ engineering. As summarized in Table 1, examples of ECM biomaterials obtained from different tissues and used in commercial scale can be given as AlloDerm® obtained from human dermis, SurgiSIS® and Restore® obtained from porcine small intestinal soft mucosa, and Synergraft® obtained from porcine heart valves [37].

Table 1: Commercial ECM products [36]

Product (Manufacturer)	Tissue Source	Application Focus
AlloDerm® (Lifecell Corp.)	Human dermis	Soft tissue
AlloPatch HD™, FlexHD® (Musculoskeletal Transplant Foundation)	Human dermis	Tendon, breast
NeoForm™ (Mentor Worldwide LLC)	Human dermis	Breast
GraftJacket® (Wright Medical Technology Inc.)	Human dermis	Soft tissue, chronic wounds
Strattice™ (Lifecell Corp.)	Porcine dermis	Soft tissue
Zimmer Collagen Repair Patch™ (Zimmer Inc.)	Porcine dermis	Soft tissue
TissueMend® (Stryker Corp.)	Bovine dermis	Soft tissue
MatriStem®, Acell Vet (Acell Inc.)	Porcine urinary bladder	Soft tissue
Oasis®, SurgiSIS® (Cook Biotech Inc.)	Porcine small intestine	Soft tissue
Restore™ (DePuy Orthopaedics)	Porcine small intestine	Soft tissue
FortaFlex® (Organogenesis Inc.)	Porcine small intestine	Soft tissue
CorMatrix ECM™ (CorMatrix® Cardiovascular Inc.)	Porcine small intestine	Pericardium, cardiac tissue
Meso BioMatrix™ (Kensey Nash Corp.)	Porcine mesothelium	Soft tissue
IOPatch™ (IOP Inc.)	Human pericardium	Ophthalmology
OrthoAdapt®, Unite® (Synovis Orthopedic and Woundcare Inc.)	Equine pericardium	Soft tissue, chronic wounds
CopiOs® (Zimmer Inc.)	Bovine pericardium	Dentistry
Lyoplast® (B. Braun Melsungen AG)	Bovine pericardium	Dura mater
Perimount® (Edwards Lifesciences LLC)	Bovine pericardium	Valve replacement
Hancock® II, Mosaic®, Freestyle® (Medtronic Inc.)	Porcine heart valve	Valve replacement
Prima™ Plus (Edwards Lifesciences LLC)	Porcine heart valve	Valve replacement
Epic™, SJM Biocor® (St. Jude Medical Inc.)	Porcine heart valve	Valve replacement

ECM can be used as a scaffold to host different cell types such as stem cells [26], or as a grafting material. The sacrificial cells which are programmed to death are allowed to secrete ECM before their death. Removal of the cells results into a porous ECM graft which can be further seeded with autologous cells [38], [27]. ECM has been used in combination with other materials in order to increase the mechanical strength and stability. To date, materials such as glutaraldehyde, genipin, and vitamin B2 were used combined with ECM for this purpose [24]. ECM materials have been used for stem cell differentiation as well, and it has been proven that ECM biomaterials have positive effects on stem cell differentiation [39].

1.2.3. Production steps of ECM biomaterials

ECM is obtained from tissues or cell cultures and needs to be processed before it can be used as a biomaterial. Such processes are usually composed of several steps that can be exemplified as but not limited to decellularization, grinding, solubilization and neutralization. The ECM can be fabricated into hydrogel in various forms such as foam, electrospinning into fibers or 3D bioprinting into more complex structures.

1.3. Decellularization Process

Decellularization is the removal of cellular content from tissues and organs, or as in our case, from the ECM structure created by the cell sheets. Decellularization can be achieved by the use of chemical or biological agents as well as by physical methods and is a crucial step in ECM biomaterial production.

Up to now, many tissues and organs such as bladder, heart valve, dermis, placenta, liver, lung and kidney have been decellularized [35]. Many different species such as mice, rats, pigs were used as tissue sources for decellularization [32]. Decellularization gains interest among researchers as it expands horizons for tissue engineering applications. An interesting example is the production of heart tissue by decellularization and recellularization of spinach tissue [40].

1.3.1. Purpose of decellularization and success criteria in decellularization

The cellular content of ECM has the potential to cause host response when grafted, therefore, has to be removed before grafting. DNA and Gal-epitope are two main reasons why host response may occur. Gal epitope, oligosaccharide α -Gal (Gal α 1,3-Gal β 1-4GlcNAc-R), is a cell membrane antigen present in all species except for Old World Monkeys and humans. As humankind do not have this antigen, the transplantation of a xenograft leads to a host reaction,

causing rejection of the graft. Therefore, the Gal epitope present on the xenografts needs to be removed before grafting [41].

As remnant DNA in the graft can cause inflammatory reactions in the host, the DNA has to be removed during decellularization. Another reason why DNA needs to be removed is that it causes calcification after implantation [35]. However, as most of the tissues are dense stacks of ECM and DNA, it is almost impossible to remove 100% of the DNA. Therefore, the remnant DNA after decellularization should be quantitatively examined, or qualitative examinations should be done, i.e. there should be no image obtained after 4',6-diamidino-2-phenylindole (DAPI) or hematoxylin and eosin (H&E) staining [36], [35]. The intracellular and cell membrane components of the cells need to be removed as well. Also, the remnant decellularization agents and immunologically active molecules are unwanted as they might cause toxicity or host response [26], [35].

Although the main aim of decellularization is the removal of the cellular content, preserving the ECM structure and composition is also important. Maximum removal of cellular content should be achieved while minimum damage caused to the ECM network. Mechanical strength and compositional integrity of the ECM structure need to be preserved [32].

1.3.2. Decellularization techniques

There are two main techniques of decellularization; immersion and perfusion methods. Depending on the type and the structure of the tissue of interest the appropriate technique should be chosen. Immersion is used when the tissue being decellularized is non-vascular while perfusion requires the vascular system for the perfusion of the decellularization agent. Immersion is applied to small, thin tissues while perfusion can be used for large tissues and organs [32]. Immersion is usually applied in combination with agitation for better diffusion of the decellularization agents to the tissue being decellularized [32].

1.3.3. Decellularization methods

All decellularization methods are based on four main steps. The first step of decellularization is to lyse the cell membrane as a preparation for the upcoming steps. This can be achieved by physical applications or by using chemicals which target the cell membrane. The second step of decellularization is the separation of cellular content from ECM structure. The third step is the solubilization of the separated cellular content. The final step is the removal of the cellular content from ECM structure. There are three main methods for decellularization: use of chemical agents, use of biological reagents and the use of physical methods [37]. As all these different methods have their advantages and disadvantages, using combinations of these methods is considered as a solution for more successful decellularization.

The selection of the appropriate method for decellularization of a certain tissue or organ depends on several variables such as the cellular content of the tissue, density and thickness of the tissue, the objective application and the desired biological and mechanical properties of the final product [26], [36].

1.3.3.1. Chemical methods

Chemical methods can effectively remove the cellular content, but at the same time, they cause loss of collagen content, and damage to the ECM structure and mechanical strength [42], [35].

Chemical agents used for decellularization are; alkaline or acid solutions, ionic detergents, non-ionic detergents and zwitterionic detergents [42]. Alkaline or acid solutions hydrolyze the cellular content and degrade the nucleic acids [26]. Sodium dodecyl sulfate (SDS) is the most commonly used ionic detergent for the successful removal of cellular content of thick tissues. Other ionic detergents used for decellularization are sodium deoxycholate and Triton X-200 [36]. Among non-ionic detergents, Triton X-100 is the most commonly used one as it provides a successful removal of cellular content. The success of Triton X-100 depends on the type of the tissue. Triton X-100 was shown successful for decellularization of thin tissues such as heart valve and blood vessel [43], [26] but unsuccessful for the decellularization of the tendon which is connective tissue. Zwitterionic detergents show properties of both ionic and non-ionic detergents [44]. These detergents are used for decellularization of thin tissues.

1.3.3.2. Biological (Enzymatic) methods

Enzymatic methods are known to remove the cellular content successfully and preserving the collagen while harming the ECM structure [37]. Biological agents used for decellularization include proteolytic enzymes, chelating agents and nucleases [26]. Chelating agents such as ethylenediaminetetraacetic acid (EDTA) and ethylene glycol tetraacetic acid (EGTA) have deleterious effects on protein-protein interactions which help to ease the decellularization process. Biological methods need to be used in combination with other decellularization methods [36].

1.3.3.3. Physical methods

Physical methods such as abrasion, sonication, and freeze-drying are useful for the disruption of the cellular membrane, and as no chemicals are used during physical decellularization methods, the risk of toxicity is eliminated. Unfortunately, this method cannot remove the cellular content completely without repetitions of the procedure which may cause the loss of protein components [35]. Therefore, the combination of physical methods with chemical and biological methods is required for complete decellularization.

1.4. 3D Bioprinting

There are many different conventional methods used for tissue engineering applications such as electrospinning, melt-molding, and freeze-drying which do not provide sufficient precision over internal and external geometry as they have control only on the bulk properties of the product [45]. Therefore, there is a great need for improved manufacturing methods which can reach the desired complexity and functionality. Three-dimensional bioprinting, an additive manufacturing method, which can overcome the problems of conventional methods, is used for the creation of such tissue constructs.

Three-dimensional bioprinting is the computer-aided fabrication of biological materials in a layer by layer manner with controlled positioning, mechanical and structural precision. The aim is creating three-dimensional tissue and organ constructs which are utilized in different fields such as tissue engineering, drug discovery, cancer research and surgical training [46]. There are multiple steps of 3D bioprinting which can be classified into three main stages as pre-process, process and post-process [47]. The first step in the pre-processing stage is the design of the geometry to be printed out. The structure to be printed out can be obtained by medical imaging techniques such as magnetic resonance imaging (MRI) and computed tomography (CT) in order

to increase the accuracy of the geometry of the product. Then, the obtained image is processed into a computer model. The generated design is sliced, and path plans are generated for each layer. The cell types and materials suitable for the targeted tissue are then selected. The printing stage is conducted with the help of computer control which increases the quality of the printed structure. The three-dimensional organization is obtained by stacking layers of two-dimensional structures where the thickness of the layers represents the resolution of the system. Lastly, during the post-process stage, the printed structure is taken into a bioreactor or an incubator for further maturation [48, 49].

1.4.1. Bioprinting methods

There are multiple acellular printing methods such as stereolithography, solid freeform fabrication and powder-fusion printing [50], but our main emphasis here is on the cell and biological material based bioprinting methods.

There are many different bioprinting methods mostly varying based on forming layers. Most commonly used bioprinting methods are extrusion based, droplet-based (inkjet) and laser-based bioprinting methods which are summarized in Figure 4. For successful bioprinting, a bioprinter should be affordable, have high resolution, full automation, user-friendliness, ease of sterilization and appropriate size [51]. Also, the printed structure should have shape fidelity, high resolution and the ability to preserve integrity when incubated with the culture medium after printing [52]. The environmental conditions such as temperature, humidity, sterilization at which the printing is being held are also important.

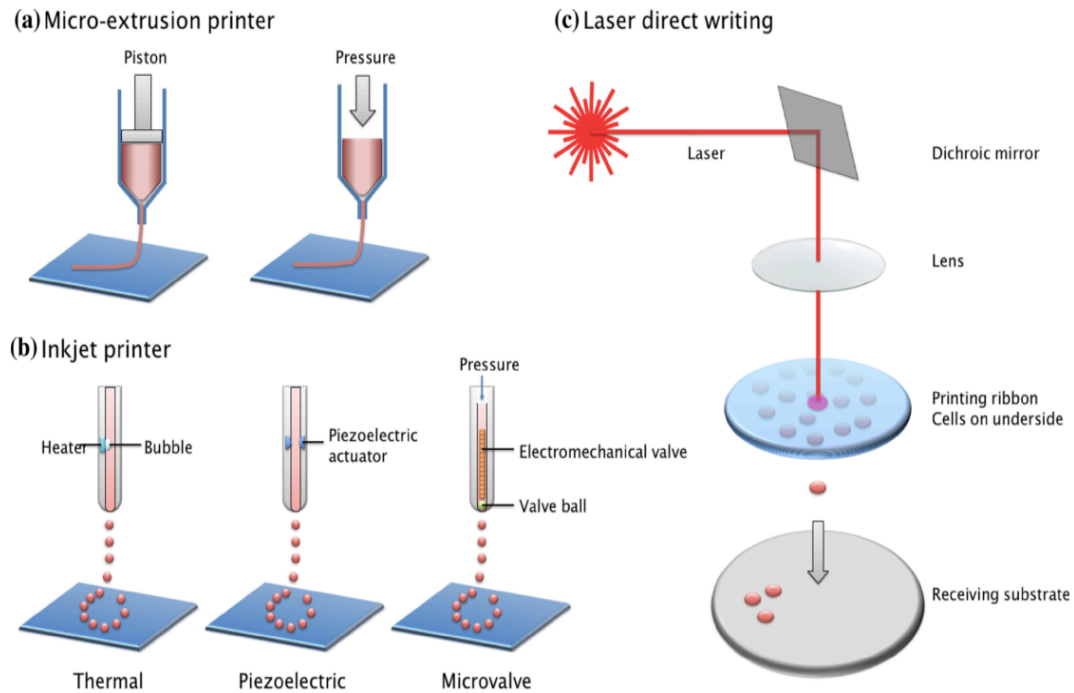


Figure 4: 3 main bioprinting methods summarized, (a) Micro-extrusion printer, (b) Inkjet printer, (c) Laser direct writing [53]

1.4.1.1. Extrusion-based 3D bioprinting

Extrusion-based bioprinting is the most popular, affordable and commercially available method of bioprinting due to its ability to print out a various number of materials and cell-friendly printing conditions [53].

During extrusion based or in other words pressure assisted 3D bioprinting, the material of interest is deposited out of the printer with the help of pressure application which is created pneumatically with an air-force pump or mechanically with mechanical screw plunger [13], [49].

The range of viscosity of the materials that are printed out with this method is very wide. Also, materials with high cell density can be printed out successfully with extrusion-based bioprinting [49]. The cell viability after printing is commonly high, very little harm is made to the cells. With extrusion based bioprinting, porous structures can also be printed [5]. The printed materials can be crosslinked chemically, thermally or with light [1]. Downsides of this method are the relatively low resolution which is around 100 μm and the low bioprinting speeds [54], [4], [50].

Most of the commercial bioprinters are extrusion based bioprinters; examples are; Bioplotter of EnvisionTec, NovoGen 3D Bioprinting Platform of Organovo [49], 3D Discovery by RegenHU as shown in Figure 5.

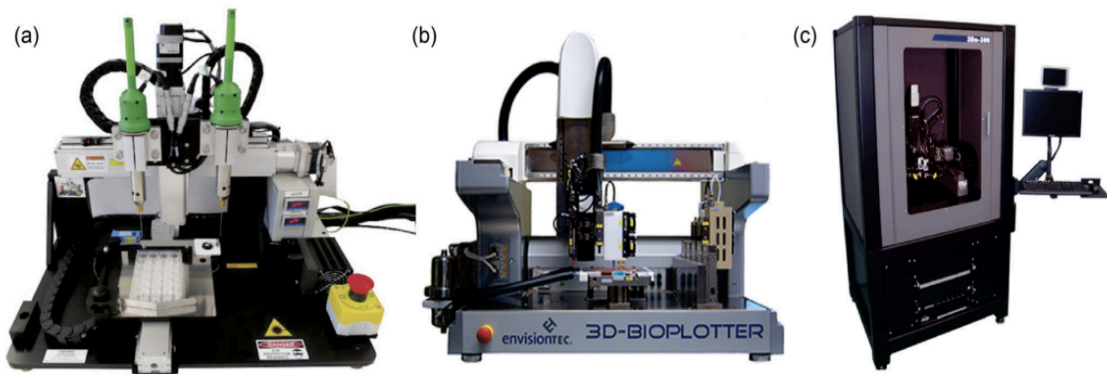


Figure 5: Widely used commercial bioprinters. (a) NovoGen 3D Bioprinting Platform of Organovo, (b) Bioplotter of EnvisionTec, (c) 3D Discovery by RegenHU [47]

1.4.1.2. Droplet-based 3D bioprinting

Droplet-based 3D bioprinting, also called drop-by-drop or drop-on-demand bioprinting, is a bottom-up process that creates three-dimensional structures by droplets of bioink generated hydrodynamically, acoustically, mechanically, electrically or thermally [4]. The most common

ways of generating the droplets are electrical and thermal manners which are classified under inkjet bioprinting [13]. During inkjet bioprinting, the bioink droplets can be generated with the help of electric charge application which leads to the vibration of piezoelectric material that forms pressure to thrust the bioink out of the nozzle in the form of droplets. This conversion between electric charge application and pressure outcome is considered as piezoelectric conversion. Another way to generate droplets is by application of temperature which leads to expansion of air bubbles and therefore, pressure increase that pushes the droplets out of the nozzle [55]. Inkjet bioprinting is the first ever used bioprinting method which originated from office type commercial inkjet printers.

In droplet-based bioprinting, the droplet volume is usually in the range of picolitres. The advantages of such systems include high resolution, ability to print materials with low viscosity, low cost, high printing speed and high cell viability [53], [49]. Also, as this is a non-contact method, where the nozzle and the surface that the printing is done on has no contact, the risk of contamination is reduced [47], [56].

Bioinks used in inkjet-based bioprinting needs to have low viscosity to be suitable for low force applications and avoiding clogging [52], [56]. As this printer requires low viscosity materials, the mechanical strength of the printed structures is relatively low [4]. Working with low viscosity materials also means that the deposition of ECM is challenging [57]. Inkjet bioprinters require temperature application which can cause stress on the cells leading to a decrease in cell viability [47]. One major drawback of inkjet bioprinters is the settling effect. At the beginning of the bioprinting process, the bioink is in a homogenous condition, but as the time passes, with the effect of gravity, cells tend to accumulate at the lower levels of the cartridge which disturbs the homogeneity and results in clogging of the printer head [58].

1.4.1.3. Laser-based 3D bioprinting

Laser-based 3D bioprinters are comprised of three main parts. The pulsed laser, the ribbon and the receiving substrate [59]. The pulsed laser helps to create the force that propels the material to the receiving substrate through the ribbon which can be considered as an energy absorbing slide [60], [49]. There are two main methods of laser-based 3D bioprinting: absorbing film-assisted laser-induced forward transfer (AFA-LIFT) and matrix-assisted pulsed laser evaporation direct writing (MAPLE-DW). The main difference between these methods is the ribbon, in the latter method, there are two layers of ribbons [60]. Laser-based printing has the advantage of reducing the risk of contamination as the nozzle of the printer does not contact the surface on which the printing is completed. This non-contact working conditions also result in increased cell viability due to little mechanical stress applied to the cells [49]. The precision and resolution are high for laser-based 3D bioprinting method [50]. Unfortunately, this system is costly and not cell friendly because of the laser beam. The laser beam is harmful to the cells and, the heat generated by the laser is another problem for cell viability.

The three methods of bioprinting are summarized in Table 2 based on most important parameters such as cost, cell viability, and resolution. The appropriate method of bioprinting needs to be selected based on the needs of the research and applications of the final construct.

Table 2: Advantages and disadvantages of different bioprinting methods summarized [4]

	Laser bioprinting	Droplet bioprinting	Extrusion bioprinting
Fabrication resolution (droplet size)	$>20\ \mu\text{m}$	$50\text{--}300\ \mu\text{m}$	$200\ \mu\text{m}$
Spatial resolution	Medium-high	Low	Medium
Preparation time	Medium-high	Low	Low-medium
Fabrication speed	Medium-fast ($200\text{--}1600\ \text{mm s}^{-1}$)	Fast ($1\text{--}10\ 000\ \text{droplet/s}$)	Slow ($10\text{--}50\ \mu\text{m s}^{-1}$)
Throughput/Scalable production	Low-medium	High	Medium
Material viscosity	$1\text{--}300\ \text{mPa s}^{-1}$	$3.5\text{--}12\ \text{mPa s}^{-1}$	$30\text{--}6 \times 10^7\ \text{mPa s}^{-1}$
Cell viability	$>95\%$	$>90\%$	$>40\text{--}95\%$
Single cell control	High	Low	Low
Cell density	Medium	Low	Medium-high
Multiple cells and Material delivery	Medium	Low-medium	Medium
Cost	High	Low	Medium

1.5. Bioinks used for 3D Bioprinting Applications

Bioink is the material that is printed out during 3D bioprinting applications. Bioinks are composed of cells, biomaterials, support materials and bioactive cues. Depending on the preferred bioprinting method and the desired properties of the product, the suitable bioink needs to be selected.

The bioinks used in 3D bioprinting needs to possess several properties such as printability, bioactivity, biocompatibility, mechanical durability, affordability, scalability, biodegradability and their microenvironment should support cell attachment, viability and proliferation in order to recapitulate the native tissues and organs [46], [42], [13], [52]. A bioink that is printable should have a large contact angle with the printing substrate. It also needs to possess tension in the vertical direction in order to keep its integrity and three-dimensional structure after the printing process [49]. A biocompatible bioink does not cause unwanted host reactions like immune response while the bioactive bioink can generate required biological responses. Mechanical durability means that the bioink is stable during and after transplantation [49].

Moreover, bioinks should not be affected by the post-printing conditions such as incubation with cell culture medium [13]. Bioinks should allow the transportation of nutrients and water as well as removal of wastes [24]. The material to be printed needs to be in aqueous or aqueous gel form in order to provide the best environment for the cells [61]. All these criteria reduce the number of the possible materials which can be used for bioprinting. There is still a need to develop new biomaterials that can fulfill the criteria above for successful, safe and efficient bioprinting. The selection of the material to be used is based on the desired properties of the final product.

1.5.1. dECM as bioink for 3D bioprinting applications

The success of dECM as bioink was shown when dECM derived from cartilage and adipose tissues were solubilized and bioprinted into PCL supporting scaffold while dECM derived from heart tissue was bioprinted without a supporting scaffold [22]. As shown in this study, dECM requires to be mixed with a mechanically stable, strong but bioinert material for mechanical success while dECM itself has the potential to improve the cellular functions such as migration, maturation, and differentiation [22]. Later on, more studies were conducted on the use of dECM as bioink. Skeletal muscle-derived dECM was used as bioink in order to fabricate skeletal muscle constructs. As most components of ECM were preserved and constructs provided appropriate support for cell viability, the skeletal muscle-derived dECM was concluded as a successful bioink [62].

Furthermore, liver-derived dECM was used as bioink. Rheological and biochemical characterizations, as well as its support for cell viability and differentiation, were tested, and the bioink was proven to be useful for tissue engineering applications [63]. Korean domestic pig skin-derived dECM was used for evaluation of a novel bioprinter and the effects of the

printing method on the printed structure. The physical properties of the bioink and cell viability were evaluated [64].

dECM lacks the mechanical properties of synthetic biomaterials as it goes through decellularization. Previously, the mechanical strength of dECM has been tried to be increased by additives such as vitamin B2 to heart derived dECM [65]. Another approach for increasing the mechanical properties of dECM bioink is blending it with conventional biomaterials. dECM has great potential to be used as blends with other materials. Since synthetic biomaterials lack bioactive properties and some of the natural biomaterials such as alginate and agarose are bioinert, combining these materials with dECM gives them required bioactive properties. At the same time, the presence of conventional material provides mechanical strength to the hybrid material [66], [13]. For example, in order to increase the cell attachment and migration of alginate, vascular tissue derived dECM was mixed with alginate and bioprinted to create blood vessel constructs. Cell proliferation, viability and differentiation evaluations showed that hybrid bioink had better properties than alginate bioink [67]. dECM hybrid bioinks are considered scalable as well as affordable when they are used as blends with other low-cost biomaterials [13].

The motivation of this thesis work is to develop a blend of cell sheet derived decellularized extracellular matrix with a conventional biomaterial, agarose for the production of a novel hybrid bioink for 3D bioprinting applications.

2. EXPERIMENTAL

2.1. Fibroblast Cell Culture

NIH 3T3 murine embryonic fibroblast cells (ATCC) were cultured in Dulbecco's Modified Eagle Medium (DMEM) with 10% fetal bovine serum (FBS) and 1% penicillin/streptomycin supplement, referred as complete medium.

To start the culture, cells were taken from the cryogenic storage tank, thawed rapidly at 37 °C water bath with rapid shakes. The melted components were transferred into 15 ml falcon tube containing a complete medium for centrifugation. Centrifugation was done at 2500 rpm for 5 minutes. After centrifugation, the supernatant was removed, the cell pellet was resuspended with 1 ml of complete medium, homogenized by aspiration and extrusion with a pipette. The suspension of cells and complete medium was transferred into 25 cm² tissue culture flask containing 4 ml of complete medium, pre-heated in the incubator. The cells were observed under a light microscope and cultured in an incubator at 37 °C with 5% CO₂. The medium was changed every three days, and the passage was done when cells reached confluency at around 85%. For passaging, the medium was emptied from the flask by aspiration, the flask was washed with PBS, and 3-4 ml of 0.25% trypsin-EDTA was added to the flask. The flask was kept in the incubator at 37 °C with 5% CO₂ for 4-5 minutes, the detachment of cells from the flask surface was controlled with the naked eye as well as under the light microscope. 3-4 ml of fresh medium was added to the flask, and the surface of the flask was washed in order to detach all of the cells. The suspension was transferred into a 15 ml falcon for centrifugation at 2500 rpm for 5 minutes. After centrifugation, the supernatant was removed, the pellet was resuspended with fresh medium, and the content was transferred into the new flask to continue cell culturing or to the six well plate for cell sheet production.

2.2. Fibroblast Cell Sheet Culture

NIH 3T3 cells (ATCC) with passage number between 10 and 12 were seeded on the six well plates with a density of 8000 cells/cm² as can be seen in Figure 6(a). The cells were cultured in Dulbecco's Modified Eagle Medium (DMEM) with 20% fetal bovine serum (FBS), 20% Ham F12 medium, 500µM of ascorbic acid and 1% penicillin/streptomycin supplement. The cells were incubated at 37 °C with 5% CO₂. The medium was changed every three days, and the cells were allowed to proliferate for five weeks until their self-detachment from the surface of the plate as can be seen in Figure 6(b) and 6(c).

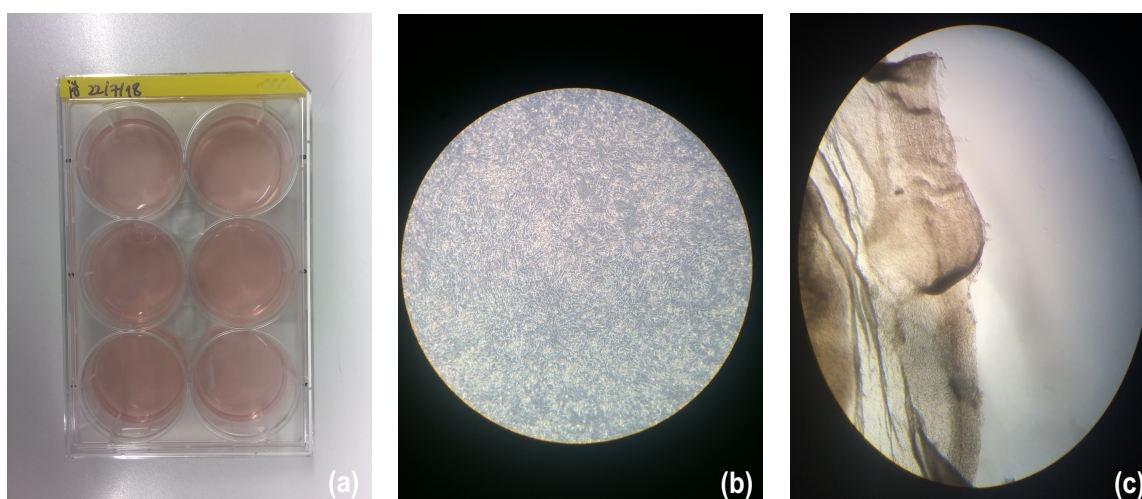


Figure 6: Fibroblast cell sheet culture (a) 3T3 fibroblast cells were seeded with 8000 cells/cm² density in 6 well plates, (b) Cells were cultured for five weeks, (c) After five weeks cell sheets detached from the surface

2.3. Preparation of Decellularization Agents

First decellularization solution including 1 M NaCl, 10 mM Tris, 5 mM EDTA was prepared by dissolving all components in 1 liter of distilled water and mixing for 30 minutes at 500 rpm. NaCl and Tris were added for osmotic shock treatment while EDTA was used for weakening the cell-cell adhesion. Second decellularization solution was prepared by dissolving 0.5 wt% SDS, 10 mM Tris, 25 mM EDTA in PBS and mixing at 500 rpm. SDS was used for solubilization of nuclear and cytoplasmic membranes as well as removal of DNA.

2.4. Decellularization of Fibroblast Cell Sheets

The cell sheets were decellularized after their self-detachment from the six well plate surface. The medium was aspirated, the first decellularization solution was added, and the plates were shaken at 75 rpm for 1 hour on a plate shaker at room temperature. After this step, the cell sheets were rinsed with PBS 3 times for 10 minutes at 75 rpm on a plate shaker. Second decellularization solution was added after the careful removal of PBS. The system was shaken for 30 minutes at 75 rpm, at room temperature. Another PBS wash step was applied, three times for 10 minutes at 75 rpm. The cell sheets were rinsed in DMEM with 20% FBS for 48 hours at room temperature at 75 rpm. The final PBS wash step was applied, for three times for 10 minutes. The obtained decellularized extracellular matrix (dECM) structures were stored in PBS at 4 °C.

2.5. Evaluation of Decellularization Protocol

2.5.1. Genomic DNA assay

The genomic DNA content of both decellularized and non-decellularized ECM samples was measured. DNA was isolated from both samples using QIAamp Fast DNA Tissue Kit. The protocol provided by the supplier was followed with minor changes based on the requirements of our work. First, the samples were freeze-dried for two days at -111 °C and 0.001 hPa in Scanvac CoolSafe Freeze Dryer. 6 mg of dECM and control (non-decellularized ECM) were weighted. The master digestion buffer including 200 µl AVE, 40 µl VXL, 1 µl DX Reagent, 20 µl Proteinase K, 4 µl RNase A (100 mg/ml) per sample was prepared. Master digestion buffer was added on samples and was vortexed for 5 minutes at full speed. No residual particles were left after this step. Then, the samples were incubated at 56 °C for 10 minutes in thermomixer at 1000 rpm. 265 µl Buffer MVL was added to both samples and mixed by pipetting. The impurities and proteins were washed off with multiple washing steps with the addition of Buffer AW1 followed by centrifugation and Buffer AW2 addition followed by centrifugation. After each step, the filtrate was discarded. On the final step of washing, 50 µl ATE was added on the samples which were in 1.5 ml sterile Eppendorf tubes, incubated for 1 minute at room temperature and centrifuged for 1 minute. The concentration of DNA in both samples were measured using NanoDrop 2000c in pedestal mode. Elution buffer was used as a blank solution.

2.5.2. DAPI staining

In order to evaluate the removal of nuclear content, dECM structures were stained with 4',6-diamino-2-phenylindole (DAPI). The ECM structures that have not been decellularized were also stained for control purposes.

The samples were fixed with 4% paraformaldehyde solution (v/v, in PBS) for 10 minutes at room temperature in the chemical fume hood. The structures were washed with PBS 3 times. The staining procedure was started with the permeabilization of the structures in 0.1 % Triton X-100 (v/v, in dH₂O) for 15 minutes at room temperature. After this step, the structures were incubated with DAPI stain prepared by 1:500 dilution of the 1 mg/ml stock solution in 1x PBS. The staining was done for 30 minutes at room temperature on a shaker. After staining, the stained structures were washed three times with PBS for 5 minutes on a shaker. The preservation of the structures was achieved with Vectashield mounting medium addition. Storage was done at 4 °C. The microscopy observations were conducted with Zeiss LSM 710 Confocal Microscope.

2.5.3. F-actin immunostaining

Cytoskeleton F-actin staining kit was used for immunostaining of both decellularized and non-decellularized ECM samples. Fixation and permeabilization of the samples were done as explained in the previous section. 1 µl of the red fluorescent phalloidin conjugate was diluted with 1 ml of labeling buffer and added to the samples. The samples were shaken in the solution for 30 minutes at room temperature. The samples were washed with PBS 2-3 times for 2-3 minutes. The stained samples were analyzed with Zeiss LSM 710 Confocal Microscope.

2.6. Characterization of dECM

2.6.1. Collagen I immunostaining

The collagen I immunostaining was done on decellularized and not decellularized ECM samples in order to observe the collagen content of both samples. The cells were fixed as discussed in the previous sections. Blocking was accomplished by incubating the samples in 3% bovine serum albumin solution (in PBS) for 90 minutes at 40 °C. Primary antibody for collagen I immunostaining was prepared with 1:500 dilution in 3% bovine serum albumin solution (in PBS). The samples were incubated with primary antibody solution at 4 °C for 12 hours. After this incubation, the samples were washed with PBS 2 times for 5 minutes. Secondary antibody (Alexa Fluor 488 conjugated goat anti-rabbit) solution was prepared as discussed for the primary antibody. Samples were incubated in this solution for 1 hour at room temperature and washed with PBS 2 times for 5 minutes. Tiled z-stack images and snap images of the stained samples were captured with Zeiss LSM 710 Confocal Microscope.

2.6.2. Fourier-Transform Infrared (FT-IR) spectroscopy analysis

FT-IR analysis was carried out on both decellularized and not decellularized ECM samples as well as SDS powder in order to show the content of both samples and the removal of the SDS used during decellularization. The removal of toxic SDS is crucial and needs to be proven before progressing into next stages of ECM processing. The FT-IR analysis is also used for observation of the effects of decellularization protocol on the protein structure of the extracellular matrix.

Both decellularized and not decellularized ECM samples were freeze-dried before FT-IR analysis. Initially, the samples were kept at -80 °C overnight. Then, the samples were dipped into liquid nitrogen for decreasing their temperature and the freeze-drying was accomplished at

-111 °C and 0.001 hPa for two days in Scanvac CoolSafe Freeze Dryer. Freeze dried samples were analyzed with FT-IR or stored at -20 °C for further use.

FTIR was done in Attenuated Total Reflection (ATR- FTIR) mode, using Thermo-Fischer Nicolet iS10 FT-IR Spectrometer. The absorbance from the air was collected before sample analysis and subtracted from the sample results as background removal. The scan number was set as 128 where the resolution was set as 4.

2.7. Preparation of dECM Hydrogel

2.7.1. Solubilization of dECM powder

dECM powders were obtained by freeze-drying for two days at -111 °C and 0.001 hPa in Scanvac CoolSafe Freeze Dryer as can be seen in Figure 7(a). The rest of the experiments were all done in safety cabinet, and UV sterilization was used before experiments for the sterilization of both the safety cabinet and the equipment such as tweezer, scissor, plate heater. Solubilization of the dECM powder was done by partial enzymatic digestion at an acidic environment. The collagen fibers were digested with the enzymatic activity of pepsin enzyme into smaller sections by hydrolyzing the peptide bonds. For this purpose, pepsin solution was prepared by adding pepsin powder from porcine gastric mucosa in 0.01 M HCl with a final concentration of 1 mg/ml. The pH of the solution was measured to be 2 where pepsin shows maximum proteolytic activity for the digestion of collagen. dECM powders were added in the pepsin solution with 10 mg dECM/mL pepsin solution concentration and were digested for 26 hours by stirring at 700 rpm at room temperature as can be seen in Figure 7(b). The digestion time was set for 26 hours where the sufficient digestion of the collagen fibers was achieved, and the excessive digestion was avoided. At the end of digestion, a flowable solution was

obtained as can be seen in Figure 7(c). The solution was stored at 4 °C for maximum one week or was used for neutralization.

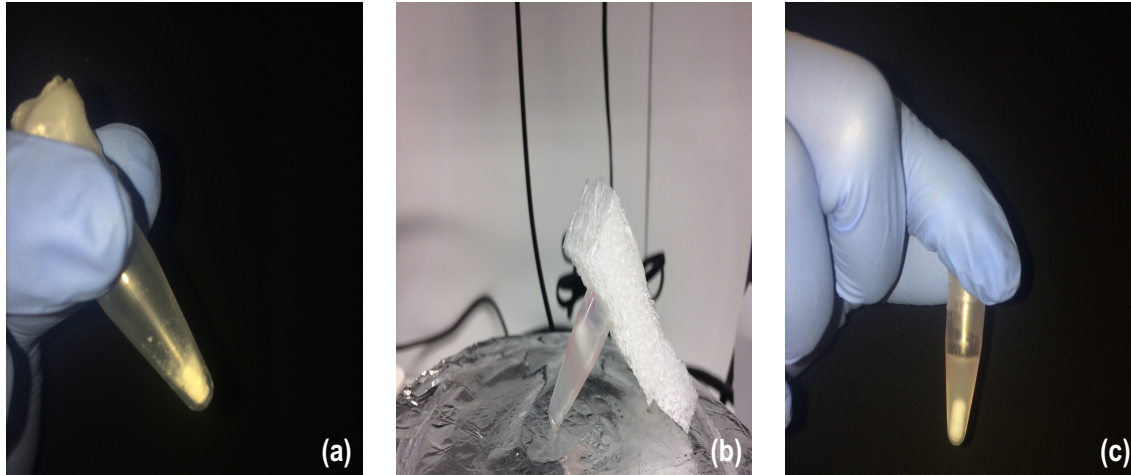


Figure 7: Steps of production of dECM gel (a) The dECM powder was obtained after freeze drying, (b) The dECM powder was digested with pepsin solution for 26 hours, (c) The digested dECM after 26 hours

2.7.2. Neutralization and sterilization of dECM solution

The digested ECM powders were pH and salt neutralized in order to initiate gelation kinetics before their use as bioink. All of the neutralization agents were stored at 4 °C before using them and the neutralization was done on ice to avoid the rapid gelation of the material. The pH neutralization was achieved by the addition of 0.1 M NaOH solution in the dECM digest in a drop by drop manner until the pH was 7.5. The pH was measured with a pH indicator after the addition of the NaOH solution. At this pH, the proteolytic activity of pepsin is stopped irreversibly, and the progress to next steps as neutralization and cell encapsulation can be done without and negative effects. The salt neutralization was obtained by addition of 10x PBS in

the solution with the final concentration of 1x. The sterilization of the material was done by addition of 1% penicillin-streptomycin in the PBS solution used for salt neutralization.

2.8. Preparation of Cell Laden dECM- Agarose Hybrid Bioink

dECM solution obtained after digestion and neutralization steps was mixed with 3% (w/v) agarose solution in 1:10 (v/v) ratio. The mixing was done at 38.5 °C to avoid gelation of the materials before printing. NIH 3T3 cells were cultured as discussed in the previous sections. The cells were mixed with agarose with 4.5×10^5 cells/ml final concentration. For the mixing of cells with agarose, cells were centrifuged in Eppendorf, the supernatant was discarded, and agarose was added on the cells by micropipette. This mixture of cells and agarose was mixed with dECM gel with the specified ratio and kept at 38.5 °C during printing. The additions and mixing were done without aspiration and extrusion to avoid creation of bubbles in the bioink. The mixing was done with 200 µl pipette tip manually.

As a control group, 3% (w/v) agarose solution was used. Due to the advantages of agarose such as being bioinert and affordable, possessing good printability and gelation, the ability to crosslink thermally and good printability, it was used in the blend bioink with dECM. Therefore, it was also used as the control group. This solution was prepared by addition of 1.5 g agarose powder into 50 ml of 1x PBS and autoclaving at 115 °C for 15 minutes. By autoclaving, the powder was dissolved in the PBS and also, the sterility of the solution was achieved. Agarose solution was prepared on the day of bioprinting and was not stored for a long time before printing to keep its properties unchanged. The same ratio of 3T3 cells was added in the agarose solution and printed under the same conditions as the hybrid bioink.

2.9. Bioprinting of Cell Laden dECM- Agarose Hybrid Bioink

For printing, an extrusion-based bioprinter, Organovo which can be seen in Figure 8 was used. The bioink was kept at 38.5 °C during printing and this temperature was continuously controlled with thermocouple to avoid decreasing in the temperature which could lead to gelation of the bioink before printing. The code needed for bioprinting was prepared according to the needs of this bioprinting. Initially, the zero point was set by moving the capillary in x, y and z-axes. Then, the bioink was aspirated from the bioink chamber with 1.5 cm length and 2 mm/s rate through a capillary with 450 µm inner and 500 µm outer diameters. Then, the bioink was chilled in 4 °C 1x PBS for 10 seconds in order to initiate gelation.

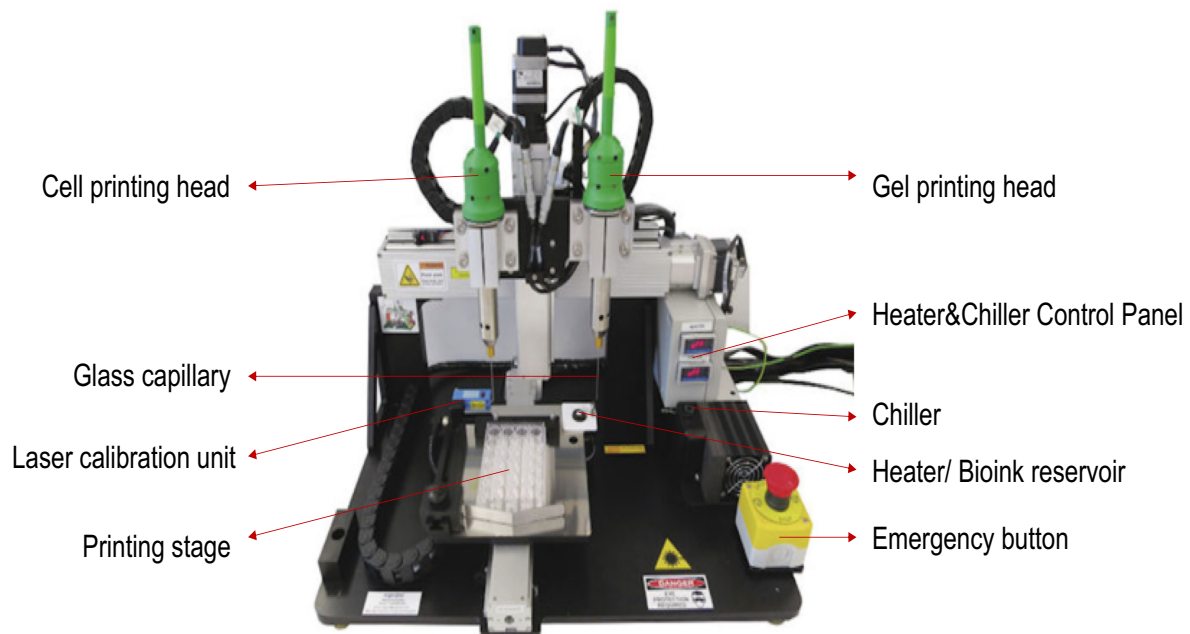


Figure 8: Organovo bioprinter parts shown

The bioprinting step is explained in detail in Figure 9. Firstly, the hybrid bioink that is kept in the bioink reservoir at 38.5 °C is aspirated with the help of the glass capillary and the moving plunger inside the capillary as can be seen in Figure 9 (a), (b) and (c) respectively. The bioink is then printed on the printing stage in stripes. The schematic figure shows printed blend dECM bioink in Figure 9 (d).

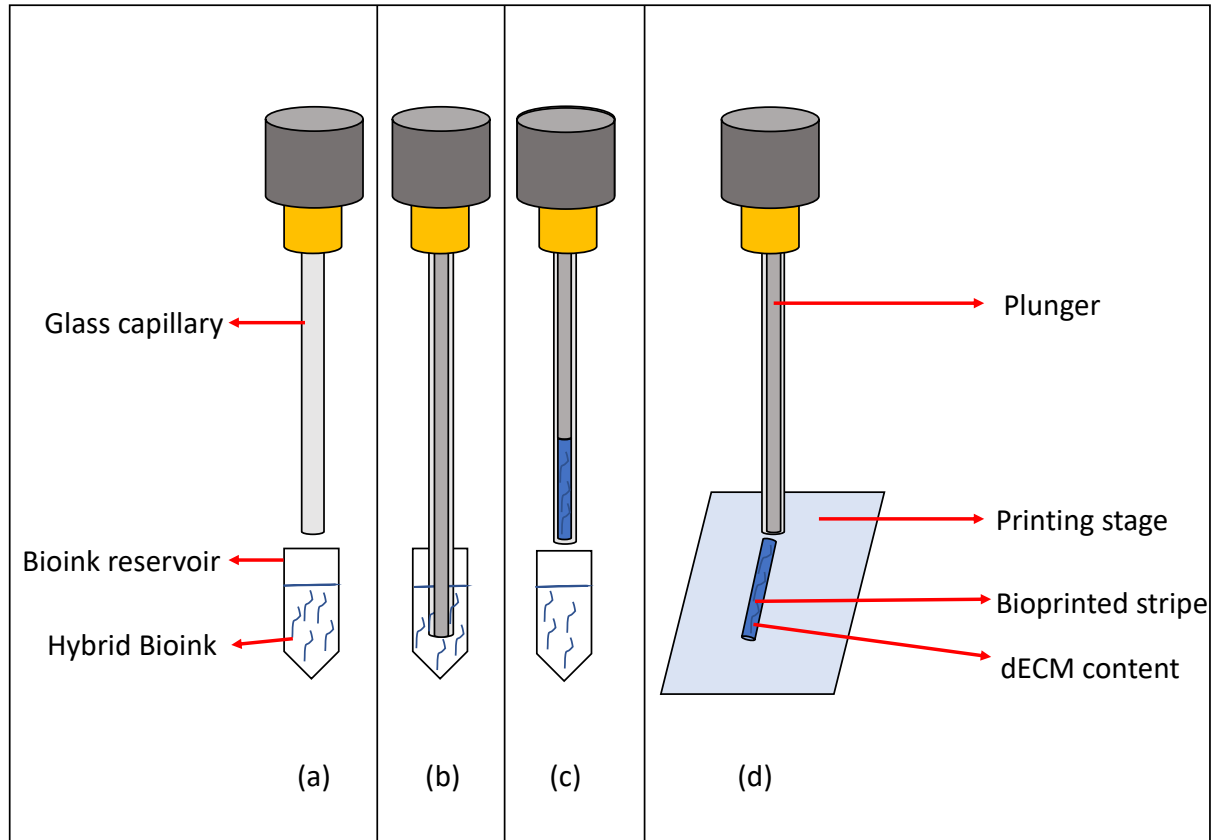


Figure 9: Bioprinting steps explained (a) System elements shown, (b) Capillary and plunger enters the bioink reservoir, (c) Aspiration of the bioink, (d) Bioprinting on the printing stage

Bioprinting of the hybrid bioink was done on agarose surface for better structural integrity and attachment to the surface as can be seen in Figure 10. The integrity of the products was preserved after bioprinting showing the ability of the material to be successfully bioprinted. Integrity preservation is a good indicator for understanding the printability of the material. After

bioprinting, the complete medium for cell culture was added on the samples, and the samples were taken to the incubator at 37 °C with 5% CO₂ level for incubation.

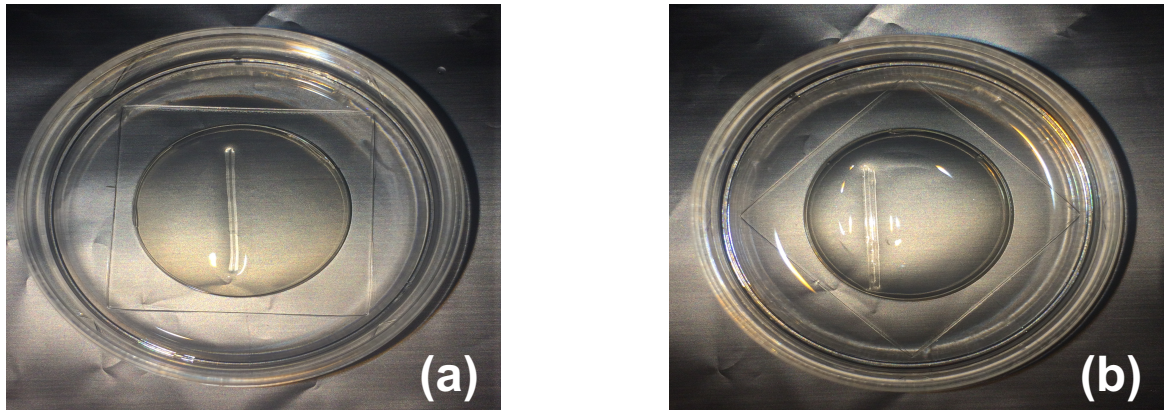


Figure 10: Bioprinted structures (a) Single stripe, (b) Three stripes printed next to each other

2.10. Live/Dead Assay

The viability of encapsulated cells in the samples was tracked and observed 0, 1, 3 and 7 days after the bioprinting with Live/Dead fluorescence assay. For this purpose, both dECM-agarose bioink and only agarose bioink samples were stained with Calcein AM and Propidium Iodide (PI). Calcein AM which was prepared by diluting a 1mg/ml stock solution in 50 μ l DMSO in dark conditions was used for detecting the living cells where PI was used for detecting the dead cells.

2 μ l Calcein AM was added in 3 ml growing medium in which the samples were and incubated for 45 minutes in the incubator at 37 °C with 5% CO₂. After incubation, the samples were washed with 1x PBS at room temperature. Then, 2.5 μ l PI was added to 3 ml of PBS which the

samples were in. The samples were incubated in the incubator at 37 °C with 5% CO₂ for 15 minutes. The stained samples were always kept in the dark, covered with aluminum foil.

As the samples were printed on a thin layer of agarose on the glass surface of 35 mm petri dish, the confocal microscopy imaging was conducted with the same dishes without the need for transferring the samples from printing dish to microscopy dish. Z stack images of the samples were taken with a Zeiss LSM 710 confocal microscope.

Quantification of the Live/Dead Assay was done by using Image J. The living, and dead cells were counted separately, the ratio of the living cells to the number of cells was calculated. These values were used as percentages and were used for understanding the cell viability.

3. RESULTS & DISCUSSIONS

3.1. Fibroblast Cell Sheet Culture and Decellularization of Fibroblast Cell Sheets

Cell sheets were cultured as discussed in the previous section and the detachment of sheets from the well plate surface was observed after five weeks of culturing. This period is shorter than what was observed in previous studies where PDMS was used as surface coating, and sheets were removed after six weeks of culturing [68]. Cell sheet detachment did not only happen in a shorter period but also required no external interference such as temperature change or enzyme treatment. This self-detachment is beneficial for the conservation of the integrity of the ECM structure.

SDS was selected as the decellularization agent as it was proven to be efficient in the removal of nuclear and cytoplasmic DNA. Decellularization of the cell sheets was accomplished by 0.5 wt% SDS containing solutions as this SDS percentage was described as high SDS concentration, 0.05 wt% SDS being the low SDS concentration, in the previous studies and proven to be leading to a more efficient DNA removal [68]. The addition and removal of all decellularization agents and PBS were done gently to reduce the harmful effects on the samples. During decellularization and washing steps, the samples were shaken at 75 rpm which is below the critical level of 100 rpm. Higher agitation speeds were proven to be harmful to ECM structure [36].

3.2. Evaluation of Decellularization Protocol

3.2.1. Genomic DNA assay

Decellularization efficiency was evaluated with Genomic DNA assay. The DNA content of two samples decellularized ECM (dECM) and non-decellularized ECM (control), were measured and the ratio of removed DNA content was used as an indicator for efficient decellularization.

In Figure 11 the DNA content of the control group is taken as 100% and compared to the decellularized ECM sample. The remnant DNA content in dECM sample is 18,9% which indicates 81,9% of the genomic DNA was removed with the decellularization protocols applied to the samples. These values show that the decellularization protocols were able to reduce the DNA content significantly when compared to the control group [69].

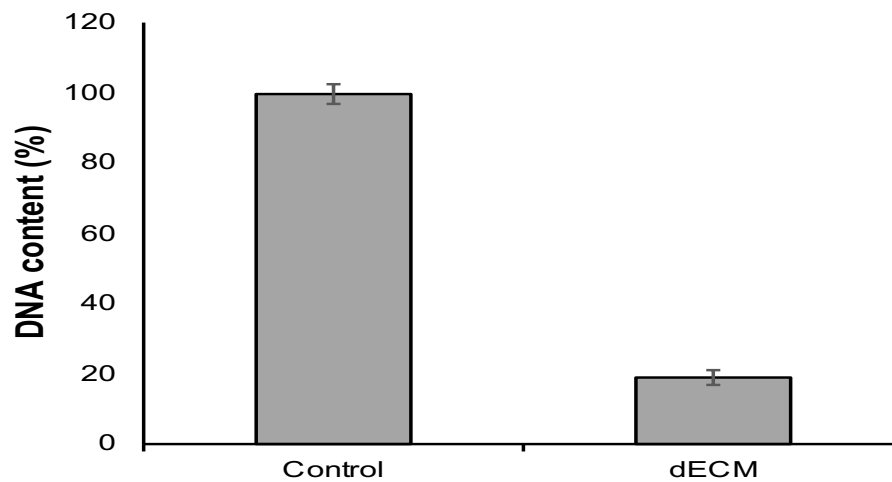


Figure 11: The DNA content comparison between non-decellularized samples (control) and decellularized samples (dECM)

3.2.2. DAPI staining and F-actin immunostaining

F-actin and DAPI staining were used for observing the structure of the cell sheets produced as can be seen in Figure 12. DAPI staining and F-actin immunostaining images also showed the removal of cell nuclei and F-actin structure in decellularized samples. As can be seen in Figure 13, while the cell sheet that has not been decellularized (control group) had clear DAPI (blue) and F-actin (red) signals, these signals were not obtained from decellularized cell sheet structures, indicating the devoid of cell nuclei and F-actin structure, respectively. In Figure 12, (a) shows the DAPI stained cell nuclei of the control group, (b) shows the F-actin structure of the control group where (c) is the merged image of both staining methods for the control group. In the lower row, the images of decellularized cell sheet are presented. No signals were obtained from DAPI staining and F-actin immunostaining of decellularized cell sheet structures as can be seen in (d) and (e) respectively. For observations of decellularized and not decellularized structures, the same digital gain inputs were used in order to have consistency among experiments.

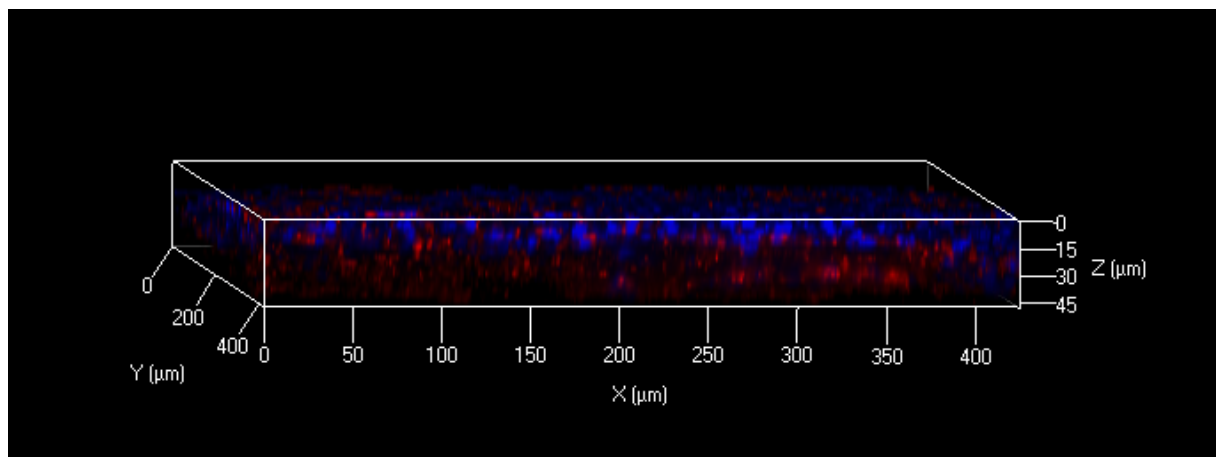


Figure 12: Cell sheet structure observed after DAPI and F-actin staining

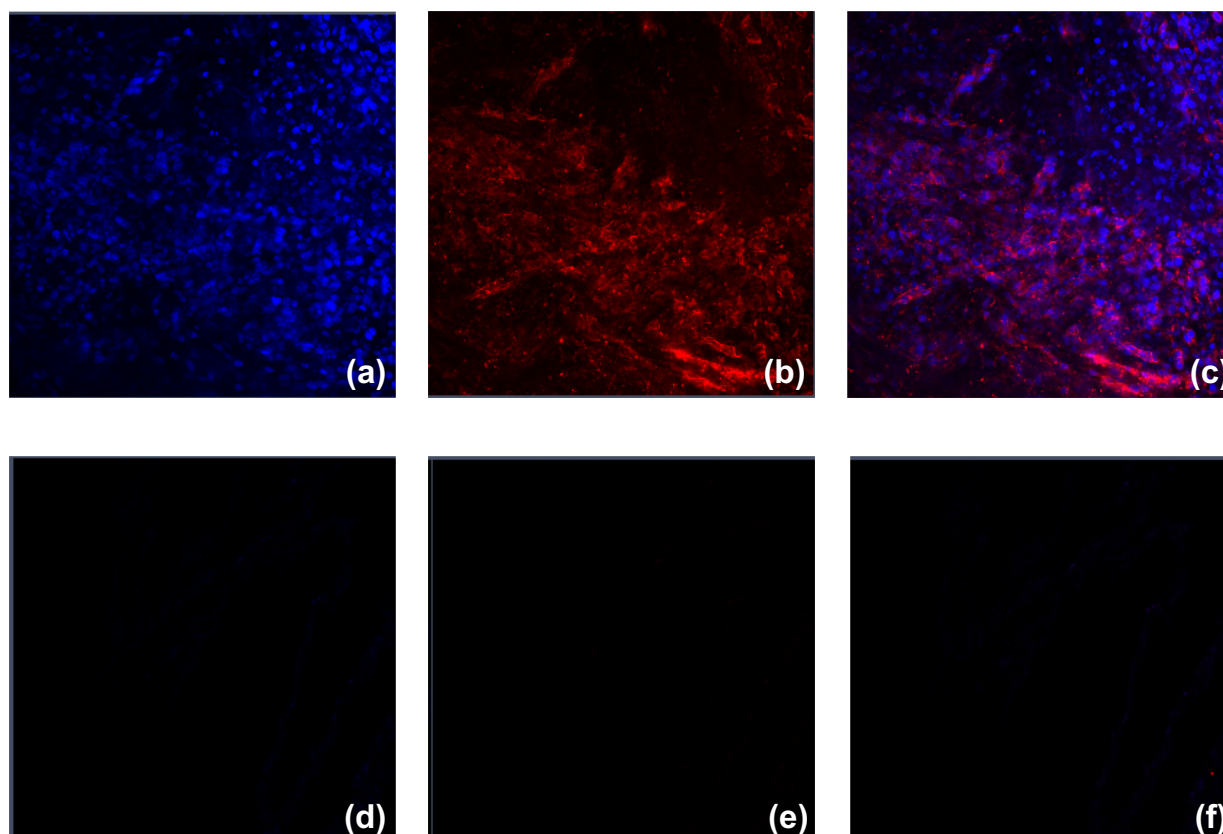


Figure 13: DAPI and F-actin staining of both decellularized and non-decellularized samples

(a) DAPI staining for control sample, (b) F-actin staining for control sample, (c) Merged image for control sample, (d) DAPI staining for dECM sample, (e) F-actin staining for dECM sample, (f) Merged image for dECM sample

3.3. Characterization of dECM

3.3.1. Collagen I immunostaining

Previous studies have proven that the most abundant protein of ECM is collagen [6]. Collagen I immunostaining was carried out in order to show this on both decellularized and not decellularized (control) samples of ECM. The collagen content was shown qualitatively on both samples as can be seen in Figure 14. In the upper row of Figure 14, the DAPI (blue) and collagen

(green) staining of the control group can be seen. The lower row shows the DAPI and collagen staining images of the decellularized ECM sample. As can be seen in (d), the cellular content is removed by decellularization successfully whereas (e) shows the conservation of the collagen content after decellularization. Figure 15 provides cross-sectional observations of both decellularized and non-decellularized cell sheets. As can be seen, the collagen content is preserved while the cells are removed after decellularization. The thickness of the samples are similar; the variations might be due to the regional folding of the sheet structure during staining and washing steps.

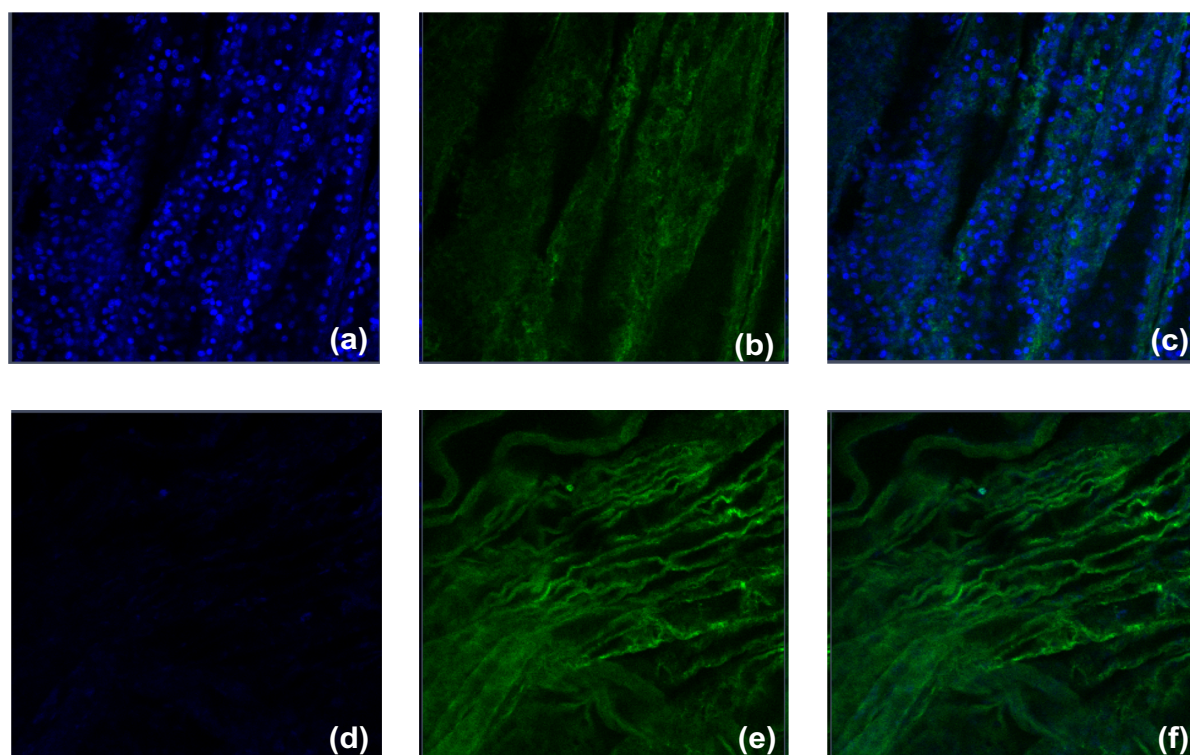


Figure 14: Collagen and DAPI staining of control and dECM samples (a) DAPI staining for control sample, (b) Collagen staining for control sample, (c) Merged image for control sample, (d) DAPI staining for dECM sample, (e) Collagen staining for dECM sample, (f) Merged image for dECM sample

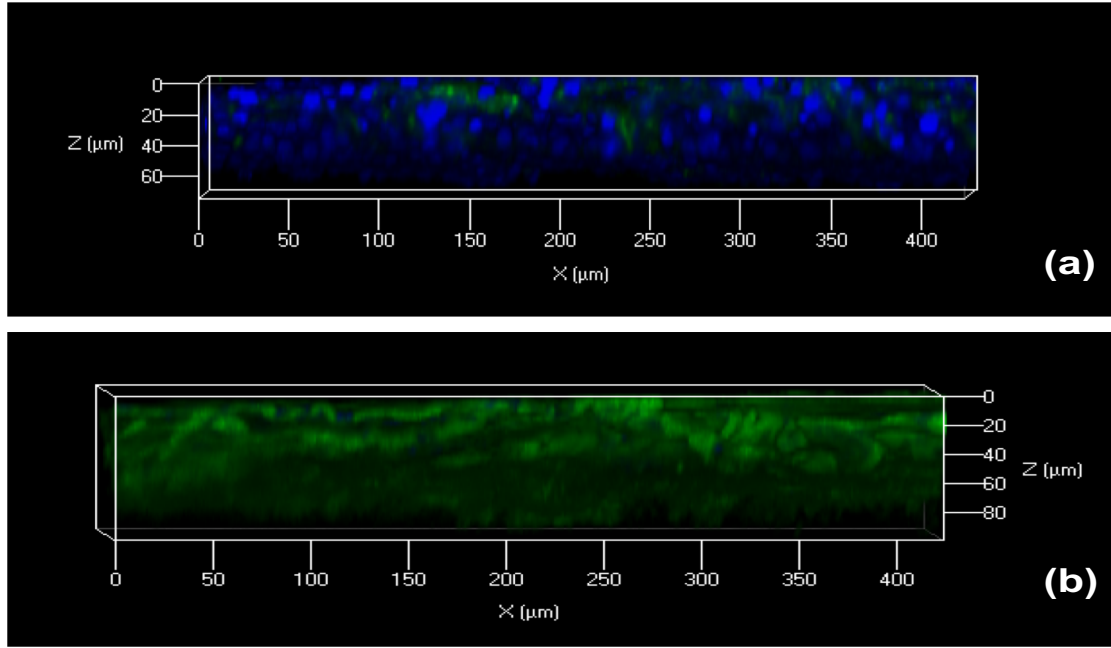


Figure 15: Cross-sectional images of DAPI and collagen staining (a) For control sample (b) for dECM sample

3.3.2. Fourier-Transform Infrared (FT-IR) spectroscopy analysis

In the FTIR analysis results, there were two main objectives. First one was to detect the absence of SDS in the decellularized samples in order to show the removal of decellularization agents was successful. SDS has sulfate groups which give characteristic peaks at 1247 cm^{-1} as we could see from FTIR results for the SDS powder in Figure 16. We expected not to see this shoulder in the dECM spectrum. As can be seen in Figure 17 and 18, there is no shoulder at 1247 cm^{-1} which means the SDS was successfully removed from the samples after decellularization. As SDS is a highly toxic material and affects the cell viability, excessive washing was applied to the samples for the removal of SDS. Therefore, it was crucial to show the removal of SDS from the samples.

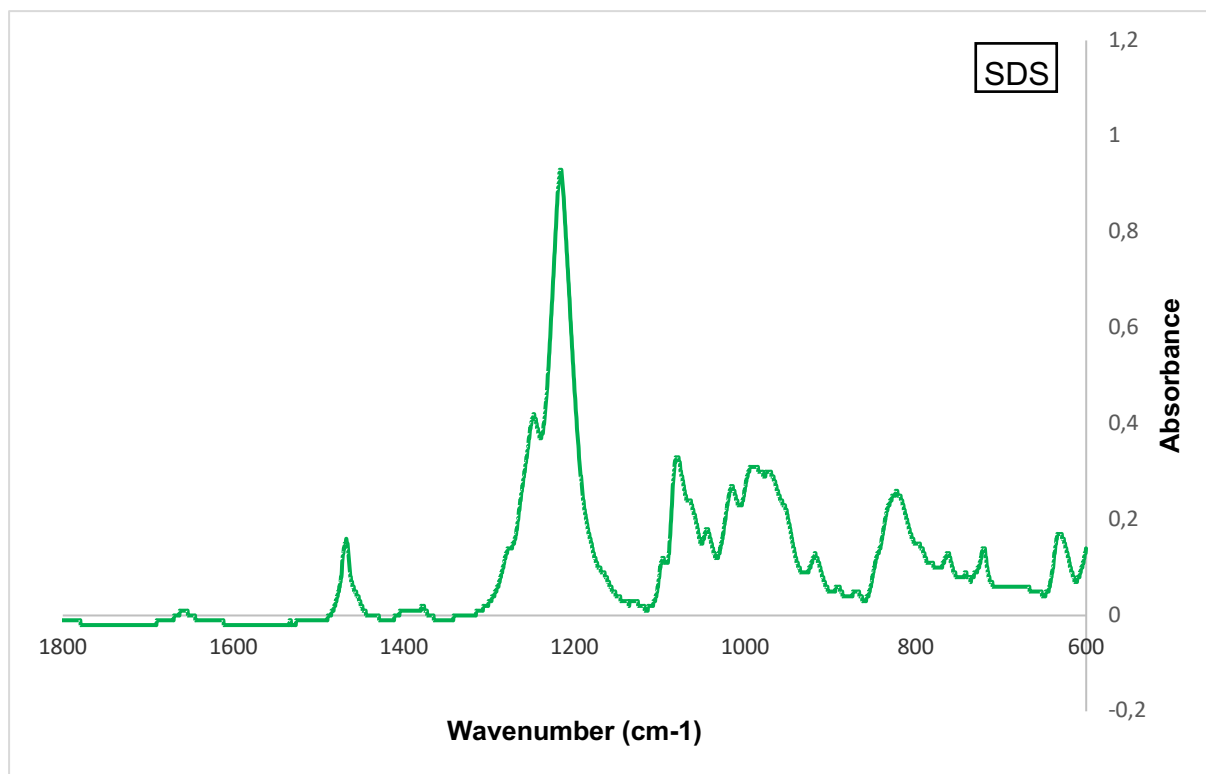


Figure 16: FTIR spectrum for SDS

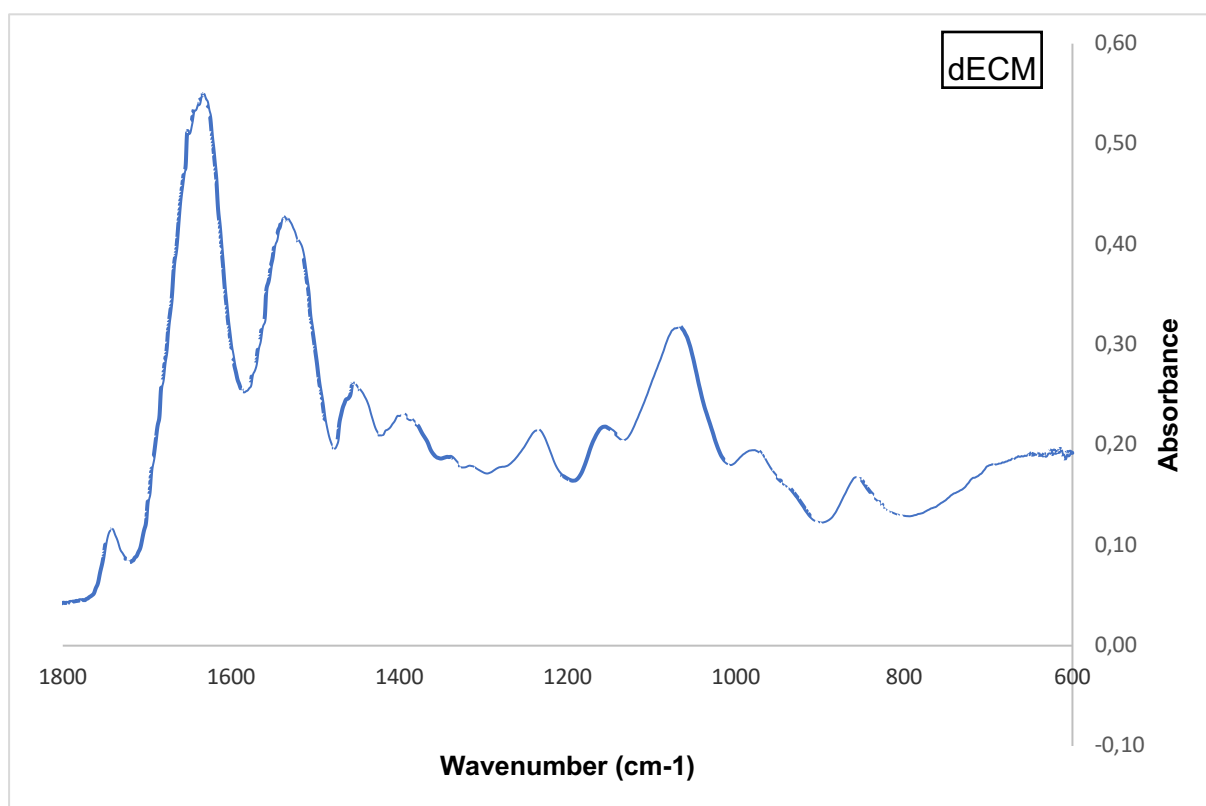


Figure 17: FTIR spectrum for decellularized ECM (dECM)

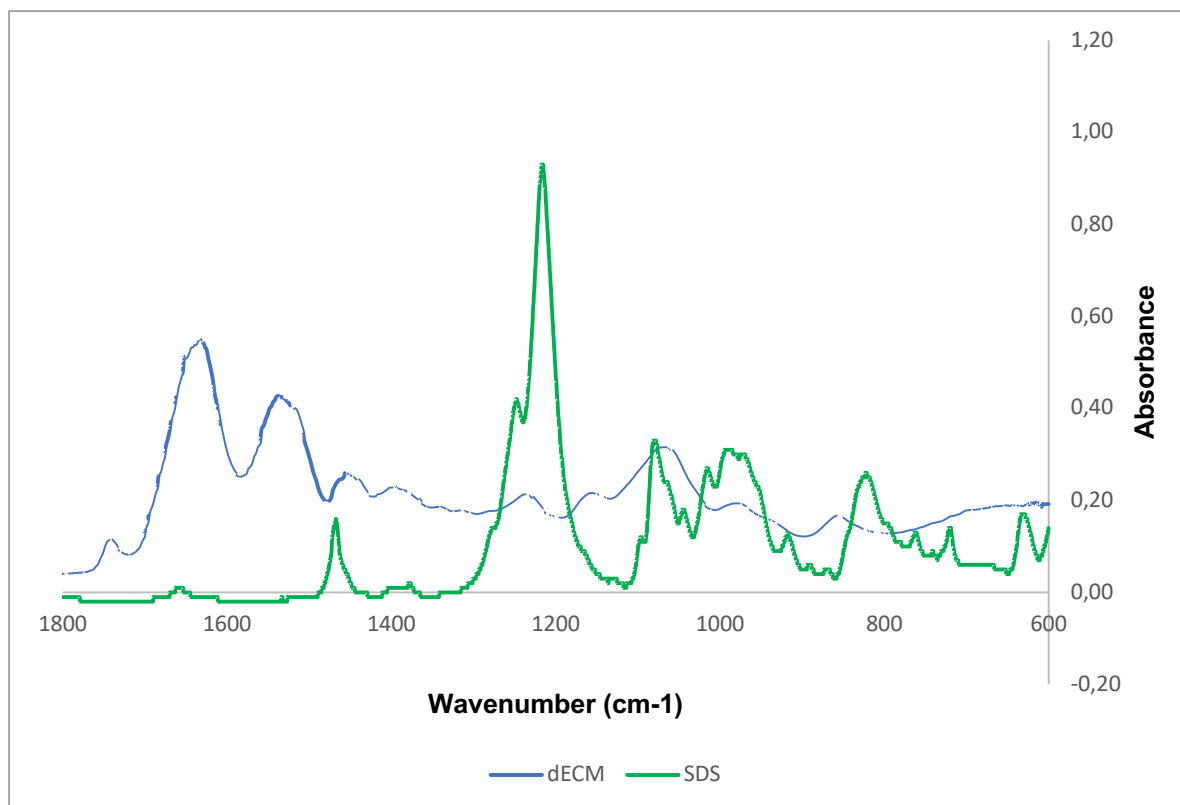


Figure 18: FTIR spectra of SDS and dECM, merged (blue line represents dECM sample, green line represents SDS sample)

Secondly, the conservation of ECM structure after decellularization was inspected. The collagen β -sheet and triple helix structures were expected to be conserved after decellularization. In order to observe this conservation, non-decellularized ECM (control) and decellularized ECM (dECM) samples were compared. As can be seen in Figure 19, the characteristic peak at 1632 cm^{-1} was observed in both samples meaning that the collagen content was conserved after decellularization.

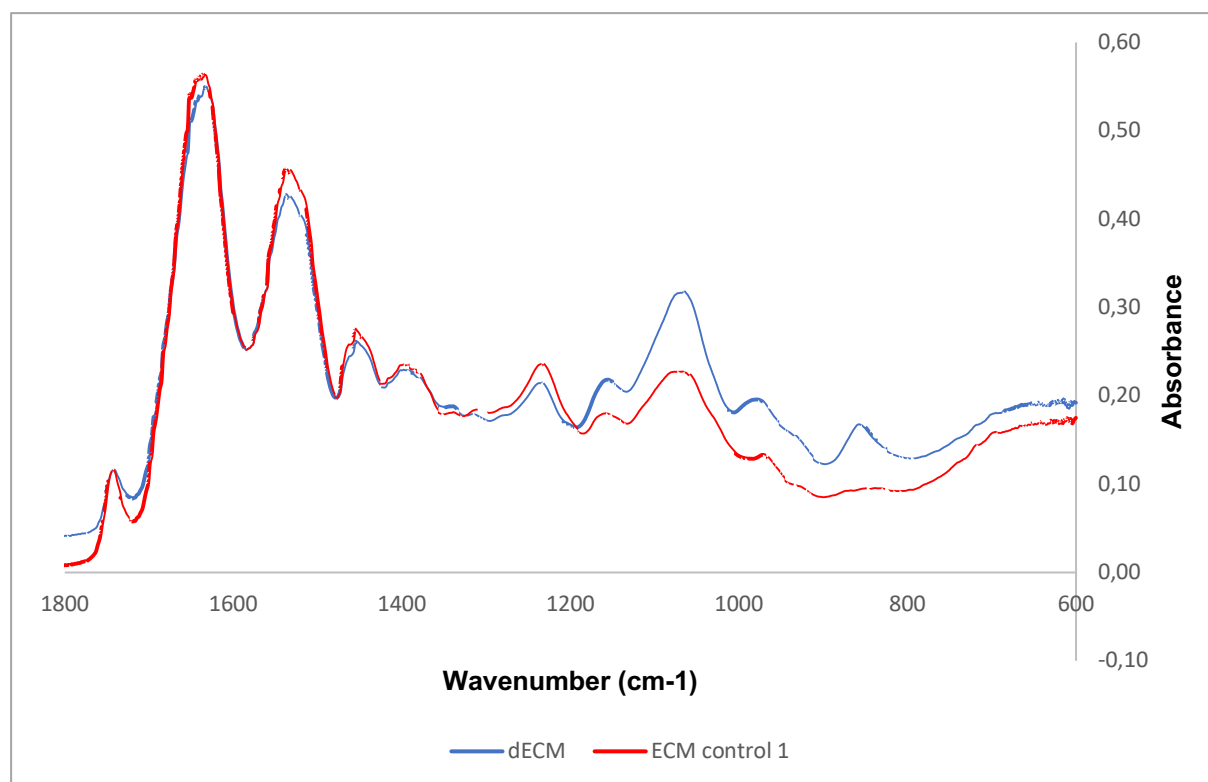


Figure 19: FTIR spectra of dECM and ECM control merged (blue line represents dECM sample, red line represents control sample)

3.4. Live/Dead Assay

The viability of 3T3 cells in both decellularized ECM-agarose-cell bioink and agarose-cell bioink (control) were evaluated 0, 1 and 7 days after the bioprinting.

The 0-day imaging was done 4 hours after the bioprinting. As agarose-cell blend was prepared by aspiration and extrusion with a micropipette, cells were homogenized better than the dECM sample where the cells were mixed in the solution by manual shaking in order to avoid bubble formation. The cell viability assay 4 hours after bioprinting showed no major difference between the control group and the dECM group as can be seen in Figure 20. One day after the bioprinting, cell viability assay was done as can be seen in Figure 21. Both of the samples had a higher ratio of dead cells compared to day 0. There was no problem of homogenous cell dispersion. As can be seen from Figure 22, Day 7 viability test showed that one week after the bioprinting, the cells in the dECM bioink showed similar cellular viability as the control group. The cells were able to attach to the material without loss of cellular viability. The high viability seen in dECM bioink samples also indicate the successful removal of SDS after decellularization as the presence of any remnant SDS would cause sudden death of cells. This result matches the results of FTIR analysis. The high viability of dECM bioink also indicates that the neutralization after pepsin digestion was completed successfully as the acidic environment is deadly for cells and if the pH were not neutralized, the cells would not show such viability.

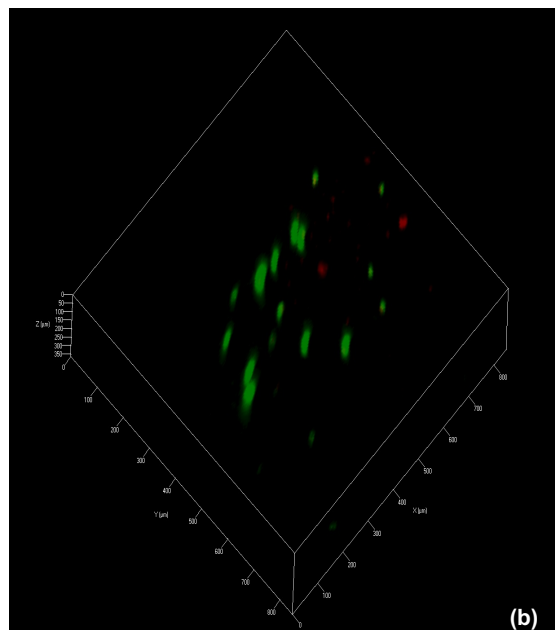
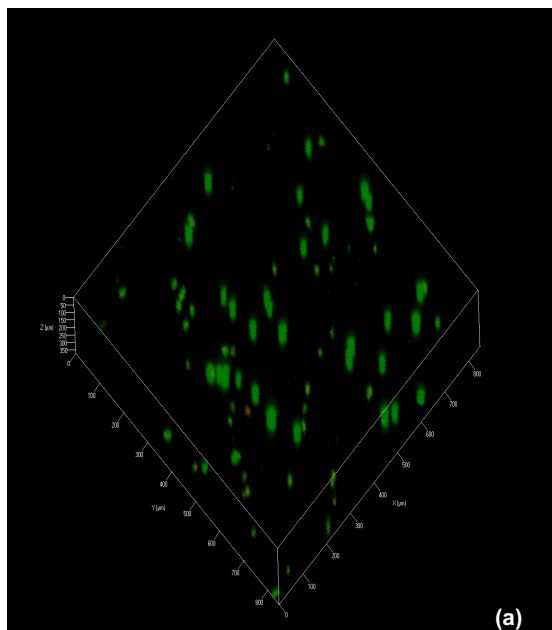


Figure 20: Live/Dead Assay Day 0, (a) control (b) dECM

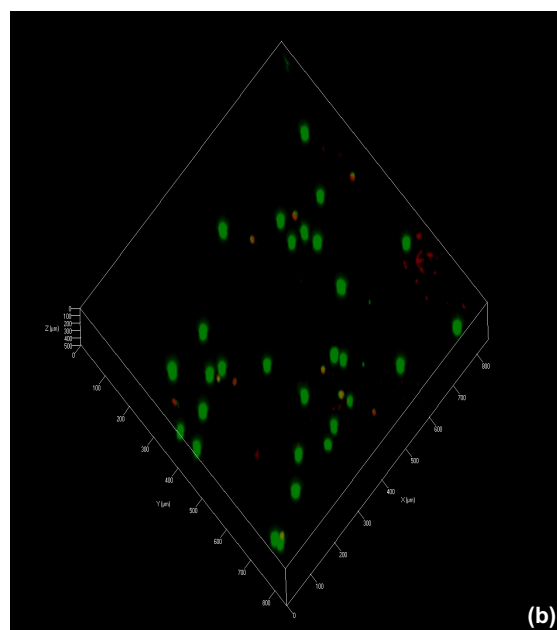
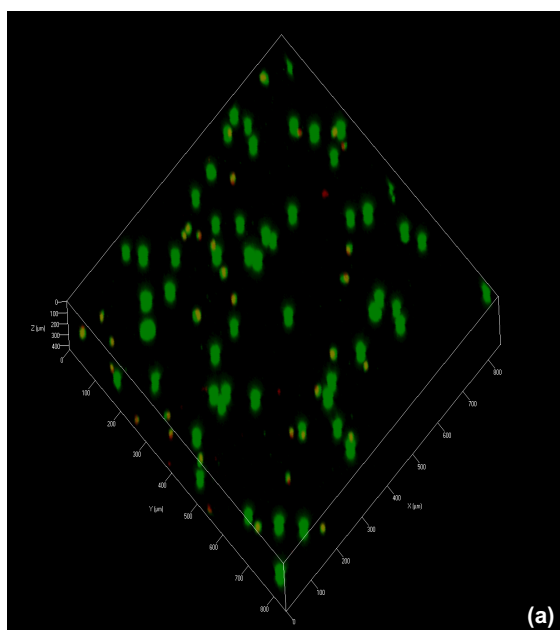


Figure 21: Live/Dead Assay Day 1, (a) control (b) dECM

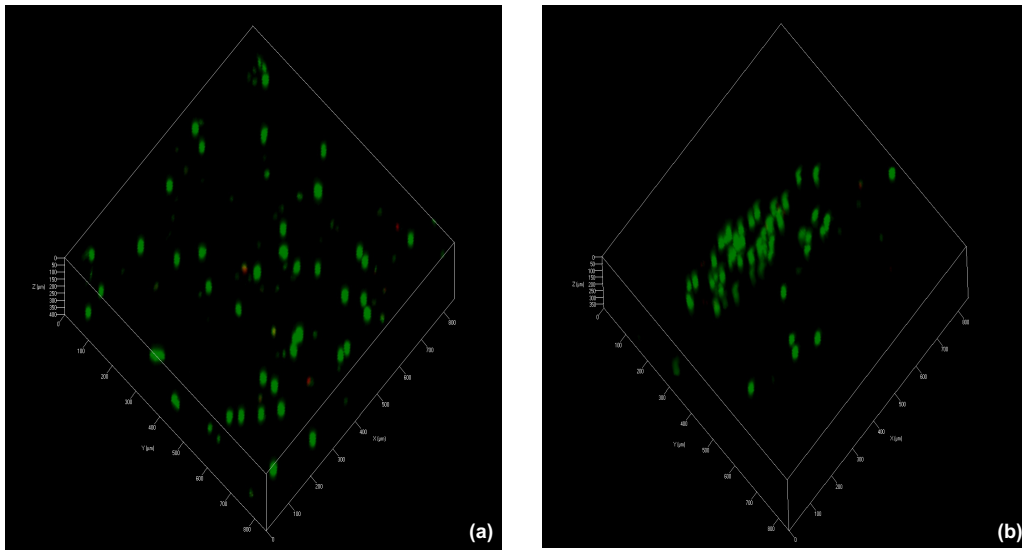


Figure 22: Live/Dead Assay Day 7, (a) control (b) dECM

The quantification of the Live/Dead assay showed that the cell viability of agarose control and the dECM- agarose hybrid bioink samples were very close 4 hours after bioprinting. The same results were achieved for day 1 and day 7 experiments. These results in Figure 23 showed the ability of dECM hybrid bioink to support the cellular viability was quite similar to the ability of agarose. The dECM bioink was able to support the cell viability, and it did not possess any toxic effect on the cells.

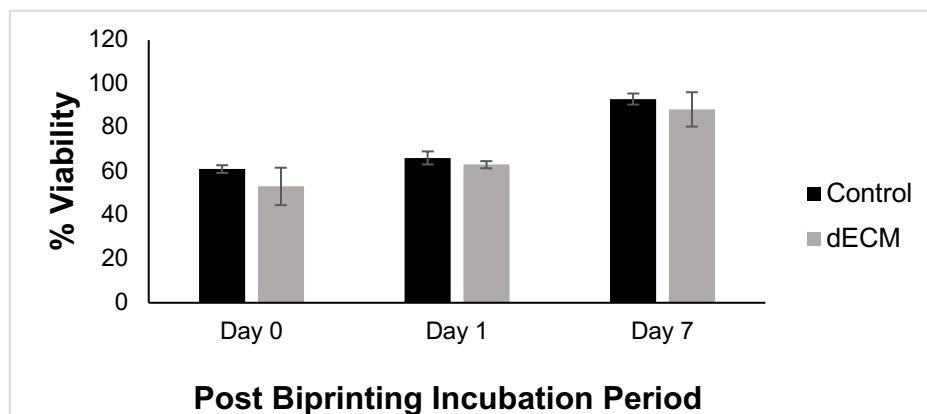


Figure 23: Quantification of Live/Dead Assay Results

4. CONCLUSION AND FUTURE WORK

The purpose of this thesis work is to produce a novel bioink which can overcome the problems faced by the current bioinks used for 3D bioprinting applications. For this purpose, a commercially available and easily printed material agarose was blended with extracellular matrix (ECM) obtained from cell sheet culturing. The cell sheets were cultured on polystyrene surface, and the detachment of the sheets was done with no enzymatic or thermal application which helps to protect the integrity of the ECM structure. Also, the cell sheets were cultured for five weeks which is a shorter period than the ones present in the literature.

After self-detachment of the cell sheets, the cellular content of the structure was removed in order to avoid unwanted host responses. For this purpose, chemical and biological agents were used. The removal of cellular content, DNA as well as the decellularization agents was evaluated and found to be successfully removed which leads to the next steps of bioink production.

Once decellularized extracellular matrix (dECM) was proven to be safe for use, it was freeze-dried into powder form, solubilized by enzymatic digestion and neutralized based on pH and salt content for providing a suitable environment for cells. The dECM gel was mixed with agarose and 3T3 cells to complete the hybrid bioink structure and printed with an extrusion-based bioprinter. The printed structures were incubated for a week with medium changes every 3 days for longer incubation and cell viability was evaluated 0, 1 and 7 days after bioprinting. The live/dead assay showed similar cellular viability among the control group and the dECM hybrid bioink showing the success of the blend bioink to support the cellular viability and causing no toxic effects.

As a future work, the dECM gel could be mixed with other hydrogels for creating different bioinks. The effect of this bioink on stem cell differentiation could be evaluated by encapsulating the cells in the bioink or by using the dECM material as a surface coating. The homogenization of the cells in the bioink is an important step that needs to be improved so both samples can be homogenized at the same quality. Other cell types such as human dermal fibroblast cells could also be used for the preparation of cell sheets in order to understand the effect of the cell line on the properties of ECM. Cell modifications could be evaluated for its possible effects on the structure, amount of ECM as well as the glycosaminoglycan content of the ECM.

REFERENCES

- [1] I. T. Ozbolat and Y. Yu, "Bioprinting toward organ fabrication: Challenges and future trends," *IEEE Trans. Biomed. Eng.*, vol. 60, no. 3, pp. 691–699, 2013.
- [2] F. A. Monibi and J. L. Cook, "Tissue-Derived Extracellular Matrix Bioscaffolds: Emerging Applications in Cartilage and Meniscus Repair," *Tissue Eng. Part B Rev.*, vol. 23, no. 4, pp. 386–398, 2017.
- [3] S. F. Badylak *et al.*, "Esophageal reconstruction with ECM and muscle tissue in a dog model," *J. Surg. Res.*, vol. 128, no. 1, pp. 87–97, 2005.
- [4] A. Arslan-yildiz, R. El Assal, P. Chen, S. Guven, F. Inci, and U. Demirci, "Towards artificial tissue models: past, present, and future of 3D bioprinting," *Biofabrication*, vol. 8, no. 1, pp. 1–17, 2015.
- [5] I. T. Ozbolat and M. Hospodiuk, "Current advances and future perspectives in extrusion-based bioprinting," *Biomaterials*, vol. 76, pp. 321–343, 2016.
- [6] P. S. Gungor-Ozkerim, I. Inci, Y. S. Zhang, A. Khademhosseini, and M. R. Dokmeci, "Bioinks for 3D bioprinting: an overview," *Biomater. Sci.*, 2018.
- [7] J. H. Park, J. Jang, J. S. Lee, and D. W. Cho, "Three-Dimensional Printing of Tissue/Organ Analogues Containing Living Cells," *Ann. Biomed. Eng.*, vol. 45, no. 1, pp. 180–194, 2017.
- [8] H. K. Makadia and S. J. Siegel, "Poly Lactic-co-Glycolic Acid (PLGA) as biodegradable controlled drug delivery carrier," *Polymers (Basel)*, 2011.
- [9] J. Malda *et al.*, "25th anniversary article: Engineering hydrogels for biofabrication," *Advanced Materials*, vol. 25, no. 36, pp. 5011–5028, 2013.
- [10] P. Serwer, J. L. Allen, and S. J. Hayes, "Agarose gel electrophoresis of bacteriophages and related particles. III. Dependence of gel sieving on the agarose preparation,"

- Electrophoresis*, vol. 4, no. 3, pp. 232–236, 1983.
- [11] R. Landers, U. Hübner, R. Schmelzeisen, and R. Mülhaupt, “Rapid prototyping of scaffolds derived from thermoreversible hydrogels and tailored for applications in tissue engineering,” *Biomaterials*, vol. 23, no. 23, pp. 4437–4447, 2002.
 - [12] D. F. Duarte Campos *et al.*, “The Stiffness and Structure of Three-Dimensional Printed Hydrogels Direct the Differentiation of Mesenchymal Stromal Cells Toward Adipogenic and Osteogenic Lineages,” *Tissue Eng. Part A*, vol. 21, no. 3–4, pp. 740–756, 2015.
 - [13] M. Hospodiuk, M. Dey, D. Sosnoski, and I. T. Ozbolat, “The bioink: A comprehensive review on bioprintable materials,” *Biotechnol. Adv.*, vol. 35, no. 2, pp. 217–239, 2017.
 - [14] S. Wüst, R. Müller, and S. Hofmann, “3D Bioprinting of complex channels - Effects of material, orientation, geometry, and cell embedding,” *J. Biomed. Mater. Res. - Part A*, vol. 103, no. 8, pp. 2558–2570, 2015.
 - [15] K. Y. Lee and D. J. Mooney, “Hydrogels for tissue engineering,” *Chem. Rev.*, vol. 101, no. 7, pp. 1869–1879, 2001.
 - [16] K. Hölzl, S. Lin, L. Tytgat, S. Van Vlierberghe, L. Gu, and A. Ovsianikov, “Bioink properties before, during and after 3D bioprinting,” *Biofabrication*, vol. 8, pp. 1–19, 2016.
 - [17] B. D. Walters and J. P. Stegmann, “Strategies for directing the structure and function of three-dimensional collagen biomaterials across length scales,” *Acta Biomaterialia*, vol. 10, no. 4, pp. 1488–1501, 2014.
 - [18] S. Van Vlierberghe, P. Dubrue, and E. Schacht, “Biopolymer-based hydrogels as scaffolds for tissue engineering applications: A review,” *Biomacromolecules*, vol. 12, no. 5, pp. 1387–1408, 2011.

- [19] A. J. Kuijpers *et al.*, “In vivo compatibility and degradation of crosslinked gelatin gels incorporated in knitted Dacron,” *J. Biomed. Mater. Res.*, vol. 51, no. 1, pp. 136–145, 2000.
- [20] Q. Xing, K. Yates, C. Vogt, Z. Qian, M. C. Frost, and F. Zhao, “Increasing mechanical strength of gelatin hydrogels by divalent metal ion removal,” *Sci. Rep.*, vol. 4, 2014.
- [21] J. W. Nichol, S. T. Koshy, H. Bae, C. M. Hwang, S. Yamanlar, and A. Khademhosseini, “Cell-laden microengineered gelatin methacrylate hydrogels,” *Biomaterials*, vol. 31, no. 21, pp. 5536–5544, 2010.
- [22] F. Pati *et al.*, “Printing three-dimensional tissue analogues with decellularized extracellular matrix bioink,” vol. 5, p. 3935, Jun. 2014.
- [23] H. Lu, T. Hoshiba, N. Kawazoe, I. Koda, M. Song, and G. Chen, “Cultured cell-derived extracellular matrix scaffolds for tissue engineering,” *Biomaterials*, vol. 32, no. 36, pp. 9658–9666, 2011.
- [24] Q. Xing, Z. Qian, W. Jia, A. Ghosh, M. Tahtinen, and F. Zhao, “Naturally Derived Extracellular Matrix for Cellular and Tissue Biomanufacturing,” *ACS Biomater. Sci. Eng.*, p. acsbiomaterials.6b00235, 2016.
- [25] H. Lu, T. Hoshiba, N. Kawazoe, and G. Chen, “Comparison of decellularization techniques for preparation of extracellular matrix scaffolds derived from three-dimensional cell culture,” *J. Biomed. Mater. Res. - Part A*, vol. 100 A, no. 9, pp. 2507–2516, 2012.
- [26] H. Hrebikova, D. Diaz, and J. Mokry, “Biomedical Papers -Epub Ahead of Print Chemical decellularization: a promising approach for preparation of extracellular matrix,” vol. 159, no. 1, pp. 12–17, 2013.
- [27] H. Lu, T. Hoshiba, N. Kawazoe, and G. Chen, “Autologous extracellular matrix

- scaffolds for tissue engineering,” *Biomaterials*, vol. 32, no. 10, pp. 2489–2499, 2011.
- [28] M. Yamato and T. Okano, “Cell sheet engineering,” *Mater. Today*, vol. 7, no. 5, pp. 42–47, 2004.
- [29] H. Takahashi, M. Nakayama, T. Shimizu, M. Yamato, and T. Okano, “Anisotropic cell sheets for constructing three-dimensional tissue with well-organized cell orientation,” *Biomaterials*, vol. 32, no. 34, pp. 8830–8838, 2011.
- [30] I. Elloumi-Hannachi, M. Yamato, and T. Okano, “Cell sheet engineering: A unique nanotechnology for scaffold-free tissue reconstruction with clinical applications in regenerative medicine,” *J. Intern. Med.*, vol. 267, no. 1, pp. 54–70, 2010.
- [31] J. C. Fitzpatrick, P. M. Clark, and F. M. Capaldi, “Effect of Decellularization Protocol on the Mechanical Behavior of Porcine Descending Aorta,” *Int. J. Biomater.*, vol. 2010, pp. 1–11, 2010.
- [32] E. Garreta *et al.*, “Tissue engineering by decellularization and 3D bioprinting,” *Mater. Today*, vol. 20, no. 4, pp. 166–178, 2017.
- [33] Y. Sheng, D. Fei, G. Leiie, and G. Xiaosong, “Extracellular Matrix Scaffolds for Tissue Engineering and Regenerative Medicine,” *Curr. Stem Cell Res. Ther.*, vol. 12, pp. 233–246, 2017.
- [34] T. Miller, M. C. Goude, T. C. Mcdevitt, and J. S. Temenoff, “Molecular engineering of glycosaminoglycan chemistry for biomolecule delivery,” *Acta Biomater.*, 2014.
- [35] M. Kawecki *et al.*, “A review of decellurization methods caused by an urgent need for quality control of cell-free extracellular matrix’ scaffolds and their role in regenerative medicine,” *J. Biomed. Mater. Res. - Part B Appl. Biomater.*, pp. 1–15, 2017.
- [36] P. M. Crapo, T. W. Gilbert, and S. F. Badylak, “An overview of tissue and whole organ decellularization processes,” *Biomaterials*, vol. 32, no. 12, pp. 3233–3243, 2011.

- [37] T. W. Gilbert, T. L. Sellaro, and S. F. Badylak, “Decellularization of tissues and organs,” *Biomaterials*, vol. 27, no. 19, pp. 3675–3683, 2006.
- [38] P. E. Bourguine, C. Scotti, S. Pigeot, L. A. Tchang, A. Todorov, and I. Martin, “Osteoinductivity of engineered cartilaginous templates devitalized by inducible apoptosis,” *Proc. Natl. Acad. Sci.*, vol. 111, no. 49, pp. 17426–17431, 2014.
- [39] K.-H. Choi, B. H. Choi, S. R. Park, B. J. Kim, and B.-H. Min, “The chondrogenic differentiation of mesenchymal stem cells on an extracellular matrix scaffold derived from porcine chondrocytes,” *Biomaterials*, vol. 31, no. 20, pp. 5355–5365, 2010.
- [40] J. Gershlak *et al.*, “Crossing kingdoms: Using decellularized plants as perfusable tissue engineering scaffolds,” *Biomaterials*, vol. 125, pp. 13–22, 2017.
- [41] S. F. Badylak and T. W. Gilbert, “Immune response to biologic scaffold materials,” *Seminars in Immunology*, vol. 20, no. 2, pp. 109–116, 2008.
- [42] B. S. Kim, H. Kim, G. Gao, J. Jang, and D. W. Cho, “Decellularized extracellular matrix: A step towards the next generation source for bioink manufacturing,” *Biofabrication*, vol. 9, no. 3, 2017.
- [43] J. Zhou *et al.*, “Impact of heart valve decellularization on 3-D ultrastructure, immunogenicity and thrombogenicity,” *Biomaterials*, vol. 31, no. 9, pp. 2549–2554, 2010.
- [44] J. S. Cartmell and M. G. Dunn, “Effect of chemical treatments on tendon cellularity and mechanical properties,” *J. Biomed. Mater. Res.*, vol. 49, no. 1, pp. 134–140, 2000.
- [45] W. Zhu, X. Ma, M. Gou, D. Mei, K. Zhang, and S. Chen, “3D printing of functional biomaterials for tissue engineering,” *Curr. Opin. Biotechnol.*, vol. 40, pp. 103–112, 2016.
- [46] S. Ji and M. Guvendiren, “Recent Advances in Bioink Design for 3D Bioprinting of

- Tissues and Organs,” *Front. Bioeng. Biotechnol.*, vol. 5, no. April, pp. 1–8, 2017.
- [47] A. B. Dababneh and I. T. Ozbolat, “Bioprinting Technology: A Current State-of-the-Art Review,” *J. Manuf. Sci. Eng.*, vol. 136, no. 6, p. 061016, 2014.
- [48] M. Guvendiren, J. Molde, R. M. D. Soares, and J. Kohn, “Designing Biomaterials for 3D Printing,” *ACS Biomaterials Science and Engineering*, vol. 2, no. 10, pp. 1679–1693, 2016.
- [49] C. Mandrycky, Z. Wang, K. Kim, and D. H. Kim, “3D bioprinting for engineering complex tissues,” *Biotechnol. Adv.*, vol. 34, no. 4, pp. 422–434, 2016.
- [50] N. A. Sears, D. R. Seshadri, P. S. Dhavalikar, and E. Cosgriff-Hernandez, “A Review of Three-Dimensional Printing in Tissue Engineering,” *Tissue Eng. Part B Rev.*, vol. 22, no. 4, pp. 298–310, 2016.
- [51] I. Donderwinkel, J. C. M. van Hest, and N. R. Cameron, “Bio-inks for 3D bioprinting: recent advances and future prospects,” *Polym. Chem.*, vol. 8, no. 31, pp. 4451–4471, 2017.
- [52] D. Chimene, K. K. Lennox, R. R. Kaunas, and A. K. Gaharwar, “Advanced Bioinks for 3D Printing: A Materials Science Perspective,” *Ann. Biomed. Eng.*, vol. 44, no. 6, pp. 2090–2102, 2016.
- [53] W. Peng, D. Unutmaz, and I. T. Ozbolat, “Bioprinting towards Physiologically Relevant Tissue Models for Pharmaceuticals,” *Trends in Biotechnology*, vol. 34, no. 9, pp. 722–732, 2016.
- [54] B. Duan, L. A. Hockaday, K. H. Kang, and J. T. Butcher, “3D Bioprinting of heterogeneous aortic valve conduits with alginate/gelatin hydrogels,” *J. Biomed. Mater. Res. - Part A*, vol. 101 A, no. 5, pp. 1255–1264, 2013.
- [55] R. R. Jose, M. J. Rodriguez, T. A. Dixon, F. Omenetto, and D. L. Kaplan, “Evolution

- of Bioinks and Additive Manufacturing Technologies for 3D Bioprinting,” *ACS Biomater. Sci. Eng.*, vol. 2, no. 10, pp. 1662–1678, 2016.
- [56] V. K. Lee and G. Dai, “Printing of Three-Dimensional Tissue Analogs for Regenerative Medicine,” *Ann. Biomed. Eng.*, vol. 45, no. 1, pp. 115–131, 2017.
- [57] S. Moon *et al.*, “Layer by Layer Three-dimensional Tissue Epitaxy by Cell-Laden Hydrogel Droplets,” *Tissue Eng. Part C Methods*, vol. 16, no. 1, pp. 157–166, 2010.
- [58] M. E. Pepper, V. Seshadri, T. C. Burg, K. J. L. Burg, and R. E. Groff, “Characterizing the effects of cell settling on bioprinter output,” *Biofabrication*, vol. 4, no. 1, 2012.
- [59] B. Guillotin *et al.*, “Laser assisted bioprinting of engineered tissue with high cell density and microscale organization,” *Biomaterials*, vol. 31, no. 28, pp. 7250–7256, 2010.
- [60] T. Jungst, W. Smolan, K. Schacht, T. Scheibel, and J. Groll, “Strategies and Molecular Design Criteria for 3D Printable Hydrogels,” *Chemical Reviews*, vol. 116, no. 3, pp. 1496–1539, 2016.
- [61] B. Derby, “Printing and prototyping of tissues and scaffolds,” *Science*, vol. 338, no. 6109, pp. 921–926, 2012.
- [62] Y. J. Choi *et al.*, “3D Cell Printing of Functional Skeletal Muscle Constructs Using Skeletal Muscle-Derived Bioink,” *Adv. Healthc. Mater.*, vol. 5, no. 20, pp. 2636–2645, 2016.
- [63] H. Lee *et al.*, “Development of Liver Decellularized Extracellular Matrix Bioink for Three-Dimensional Cell Printing-Based Liver Tissue Engineering,” *Biomacromolecules*, vol. 18, no. 4, pp. 1229–1237, Apr. 2017.
- [64] G. Ahn *et al.*, “Precise stacking of decellularized extracellular matrix based 3D cell-laden constructs by a 3D cell printing system equipped with heating modules,” *Sci.*

- Rep.*, vol. 7, no. 1, pp. 1–11, 2017.
- [65] J. Jang, T. G. Kim, B. S. Kim, S. W. Kim, S. M. Kwon, and D. W. Cho, “Tailoring mechanical properties of decellularized extracellular matrix bioink by vitamin B2-induced photo-crosslinking,” *Acta Biomater.*, vol. 33, pp. 88–95, 2016.
 - [66] M. P. Lutolf and J. A. Hubbell, “Synthetic biomaterials as instructive extracellular microenvironments for morphogenesis in tissue engineering,” *Nature Biotechnology*, vol. 23, no. 1, pp. 47–55, 2005.
 - [67] G. Gao *et al.*, “Tissue Engineered Bio-Blood-Vessels Constructed Using a Tissue-Specific Bioink and 3D Coaxial Cell Printing Technique: A Novel Therapy for Ischemic Disease,” *Adv. Funct. Mater.*, vol. 27, no. 33, pp. 1–12, 2017.
 - [68] Q. Xing, K. Yates, M. Tahtinen, E. Shearier, Z. Qian, and F. Zhao, “Decellularization of fibroblast cell sheets for natural extracellular matrix scaffold preparation.,” *Tissue Eng. Part C. Methods*, vol. 21, no. 1, pp. 77–87, 2015.
 - [69] K. Xu *et al.*, “Efficient decellularization for tissue engineering of the tendon-bone interface with preservation of biomechanics,” *PLoS One*, 2017.